

All-sky Co-moving Recovery Of Nearby Young Members. (ACRONYM) II: The β Pictoris Moving Group¹

Evgenya L. Shkolnik

School for Earth and Space Exploration, Arizona State University, Tempe, AZ, 85281 USA

shkolnik@asu.edu

Katelyn N. Allers²

Department of Physics and Astronomy, Bucknell University, Lewisburg, PA 17837, USA

Adam L. Kraus

Department of Astronomy, The University of Texas at Austin, Austin, TX 78712, USA

Michael C. Liu²

Institute for Astronomy, University of Hawaii at Manoa, 2680 Woodlawn Dr., Honolulu, HI 96822, USA

and

Laura Flagg

Physics & Astronomy Department, Rice University, 6100 Main MS-550, Houston, TX 77005, USA

Department of Physics and Astronomy, Northern Arizona University, Flagstaff, AZ, 86011 USA

ABSTRACT

We confirm 66 low-mass stellar and brown dwarf systems (K7-M9) plus 19 visual or spectroscopic companions of the β Pictoris Moving Group (BPMG). Of these, 41 are new discoveries, increasing the known low-mass members by 45%. We also add four objects to the 14 known with masses predicted to be less

¹Based on observations made with the IRTF, Keck and Magellan/Clay telescopes.

²Visiting Astronomer at the Infrared Telescope Facility, which is operated by the University of Hawaii under contract NNH14CK55B with the National Aeronautics and Space Administration.

than $0.07M_{\odot}$. Our efficient photometric+kinematic selection process identified 104 low-mass candidates which we observed with ground-based spectroscopy. We collected infrared observations of the latest spectral types ($>M5$) to search for low gravity objects. These and all $<M5$ candidates were observed with high-resolution optical spectrographs to measure the radial velocities and youth indicators, such as lithium absorption and $H\alpha$ emission, needed to confirm BPMG membership, achieving a 63% confirmation rate. We also compiled the most complete census of the BPMG membership with which we tested the efficiency and false-membership assignments using our selection and confirmation criteria. We assess a group age of 22 ± 6 Myr using the new census, consistent with past estimates. With the now densely sampled lithium depletion boundary, we resolve the broadening of the boundary by either an age spread or astrophysical influences on lithium burning rates. We find that 69% of the now known members with AFGKM primaries are M stars, nearing the expected value of 75%. However, the new IMF for the BPMG shows a deficit of $0.2\text{--}0.3M_{\odot}$ stars by a factor of ~ 2 . We expect that the AFGK census of the BPMG is *also* incomplete, probably due to biases of searches towards the nearest stars.

Subject headings: binaries: spectroscopic open clusters and associations: individual (β Pictoris Moving Group) stars: kinematics and dynamics stars: low-mass stars: pre-main sequence

1. Introduction

The discoveries of young moving groups (YMGs) throughout the past two decades have provided samples of young, nearby stars (e.g. Kastner et al. 1997; Webb et al. 1999; Torres et al. 2000; Zuckerman & Webb 2000; Zuckerman & Song 2004; Shkolnik et al. 2012; Malo et al. 2013, 2014a; Kraus et al. 2014; Aller et al. 2016) for studies of star formation, stellar evolution, and activity-rotation-age relations. They also serve as prime targets for direct imaging searches for circumstellar disks, close stellar and brown dwarf (BD) companions and young exoplanets. These groups most likely formed in coeval, co-spatial, and co-moving molecular clouds and then spatially dispersed over time, now linked through their common space motion and indications of youth. Two of the youngest such groups are the 8–10 Myr (Barrado Y Navascués 2006; Bell et al. 2015) TW Hya Association (TWA; Webb et al. 1999; Zuckerman et al. 2001b) named for the isolated T Tauri star, and the 20–25 Myr (Binks & Jeffries 2014; Malo et al. 2014a; Mamajek & Bell 2014; Bell et al. 2015) β Pic moving group (BPMG; Zuckerman et al. 2001a; Zuckerman & Song 2004; Torres et al. 2006, 2008;

Schlieder et al. 2010, 2012a,b), named for its debris-disk and exoplanet hosting hot star.

Surveys for young and active stars have revealed ≈ 10 additional YMGs with ages between 8 and 300 Myrs, filling a critical age gap between the very young star-forming regions and the old field population (Mamajek 2016). The close proximity to these YMG members to Earth ($\lesssim 100$ pc) is also beneficial for studies in need of high angular resolution, such as circumstellar disk and planet imaging, and sensitivity to low-mass stellar and substellar companions. At these young ages, disks and planets are also at their brightest and more easily detectable, e.g. the well-studied AU Mic debris disk (Liu 2004; Boccaletti et al. 2015) and substellar companions (Delorme et al. 2012; Bowler et al. 2013, 2015b).

In this paper, we present the *All-sky Co-moving Recovery Of Nearby Young Members* (ACRONYM) of the BPMG, the second in our series of YMG member searches, after our first paper on the 40-Myr Tuc-Hor YMG (Kraus et al. 2014). Early literature values of the age of the BPMG were ≈ 12 Myr for over a decade (Table 1 of Mamajek & Bell 2014). More recent work including lithium and isochrone analyses have converged to an age of 23 ± 3 Myr (Binks & Jeffries 2014; Bell et al. 2015). By 23 Myr, the stars will likely have already formed their giant planets and are in the process of forming terrestrial planets (Lissauer 1987; Pollack et al. 1996; Kenyon & Bromley 2006). Currently, there are two directly imaged planets known around BPMG members: a ≈ 7 M_{Jup} planet around its namesake A0 star, β Pic (Lagrange et al. 2010), and a 2.5 M_{Jup} planet around the F0 star, 51 Eridani (Macintosh et al. 2015). There is also one known free-floating planetary mass L dwarf PSO J318.5338-22.8603 (Liu et al. 2013; Allers et al. 2016). Smaller planets have not yet been found around such young stars primarily due to the detection limitations of direct imaging instruments and radial velocity (RV) searches. We focused our search on new low-mass members (K7-M9; $M_* \lesssim 0.7M_\odot$) around which most planets form and contrast ratios are more favorable for directly imaging planets and low-mass companions.

Prior to this publication, there were 146 systems confirmed as BPMG members consisting of 16 systems with A or F star primaries, 33 with G or K primaries, 80 M star (M0-M6) systems, and 14 brown dwarfs ($\geq M7$), yielding a 61% M-star fraction of the AFGKM stars. (See Appendix for complete census.¹) Yet, with M dwarfs making up 75% of the stellar mass function in the field (Bochanski et al. 2010), we expected that ~ 75 of the low-mass members of BPMG had yet to be discovered. In this paper, we report the confirmation of 66 low-mass BPMG members, 41 of which are new discoveries (37 M stars + 4 BDs), increasing the known M-star fraction to 69%.

¹Three BPMG members do not have published spectral types.

2. Photometric Candidate Selection

Our photometric selection process to identify BPMG candidates and the spectroscopic analysis needed for confirmation of new members are nearly identical to those used in our search for new Tuc-Hor moving group members (Kraus et al. 2014). To summarize, we combined astrometry and photometry from USNO-B1.0 (Monet et al. 2003), 2MASS (Skrutskie et al. 2006), SDSS DR9 (Ahn et al. 2012), DENIS (Epchtein et al. 1994) and UCAC3 (Zacharias et al. 2010). These data yielded proper motions from the astrometry, and spectral types (SpT) and bolometric fluxes from SED fitting of the photometry for all sources in those catalogs. To concentrate our search on the most probable candidates, we narrowed our input sample using two spatial cuts. First, to avoid crowding and its effects on the inferred stellar properties, we neglected sources near the galactic plane and center ($|b| < 5^\circ$, or $|b| < 10^\circ$ and $310^\circ < l < 50^\circ$). Second, to focus our consideration to the locus of known BPMG members (Figure 1), we disregarded targets with $7h < \alpha < 18h$.

Nearly all of the sources that passed our two selection criteria have proper motions or color-magnitude diagram positions inconsistent with membership in the BPMG, so they were winnowed to find the small number of bona fide members. We first computed the kinematic distance modulus (DM_{kin}) that would minimize the difference between a source’s observed proper motion and the expected proper motion for a BPMG member at that position on the sky. The magnitude of this discrepancy is reported as Δ_{PM} . We identified 4486 sources where the observed and expected proper motions agreed within 3σ (i.e., $\Delta_{PM}/\sigma_\mu < 3$) or the total discrepancy was $\Delta_{PM} < 10$ mas/yr, and the inferred kinematic distance was $d \leq 65$ pc ($DM_{kin} \leq 4.0$). We then estimated the height above the main sequence by comparing the kinematic distance modulus to the spectrophotometric distance modulus, requiring $0.5 \leq (DM_{kin} - DM_{phot}) \leq 4.0$ to select pre-main sequence stars. The HR diagram criterion reduced our target list to 660 photometric+kinematic candidates. Finally, we narrowed our focus to the 104 candidates with SpTs of K7–M9. The SpT for each star was measured from the SED fitting process (SpT_{SED}) described by Kraus et al. (2014). In that paper, we showed that they are consistent with SpTs measured from optical spectra for $K7 \leq SpT \leq M5.5$. Candidates with SpT_{SED} later than M5 were targeted with IR spectroscopy (Section 3) to search for indications of low-gravity. Those candidates that appeared low-gravity and all those with $SpT_{SED} < M5$ were observed with optical spectroscopy. We measured the spectroscopic SpTs (SpT_{spec}) from the IR and/or optical data when possible, which are usually consistent to within one subclass for stars later than K7. In a few cases, poor seeing did not allow for a reliable narrow-band TiO index to be measured (Shkolnik et al. 2009).

Several studies have demonstrated that new members of YMGs also can be identified using ultraviolet photometry from *GALEX* (Findeisen & Hillenbrand 2010; Shkolnik et al.

2011; Rodriguez et al. 2011, 2013). A test of this selection process in our Tuc-Hor search (Kraus et al. 2014) showed that applying a *GALEX* selection criterion to candidates is indeed more efficient, leading to a higher confirmation rate for spectroscopic follow-up. However, *GALEX* only provides coverage of 2/3 of the sky (excluding the galactic plane), so $\approx 33\%$ of unknown members would not be confirmed. Our photometric+kinematic selection procedure is unbiased toward stellar activity. Although the process requires the collection of more spectra of candidates, it will ultimately discover 50% more members with a small reduction in efficiency, i.e. 78% with *GALEX* pre-selection compared to $\approx 67\%$ without for the Tuc-Hor sample.

We list the 104 late-type candidate members of the BPMG in Table 1 with their relevant photometric and kinematic information, as well as a log of the spectroscopic follow-up observations.

3. Near-Infrared Spectroscopy of Late-M Candidates

After photometric candidate selection, spectroscopic observations are necessary to assess youth. Spectroscopic youth indicators include features of low gravity, strong H α emission, and Li absorption. For our faintest and latest SpT candidates, we first vetted for signs of low-gravity with lower-resolution near-IR spectra before collecting high-resolution optical spectra.

We obtained near-IR spectra of the 43 candidates with SED-fit spectral types \gtrsim M4 using SpeX, the facility spectrograph of the NASA Infrared Telescope Facility (IRTF) on Mauna Kea. We searched for signatures of low gravity in their spectra and re-measured their SpTs to confirm those determined by SED fitting using the method of Allers & Liu (2013), hereinafter AL13. Our near-IR and SED spectral types agree well (to within one subclass). Spectra were reduced using Spextool² (Cushing et al. 2004), which includes a correction for telluric absorption (Vacca et al. 2004).

We classified our spectra following the method of AL13. We determined gravity-insensitive near-IR spectral types using visual comparison with spectral standards from Kirkpatrick et al. (2010) as well as the spectral indices from AL13. We then calculated the AL13 gravity-sensitive indices for each spectrum and determined gravity classifications. The results are listed in Table 2. Fifteen targets had near-IR spectral types earlier than M5, for which the AL13 gravity classification cannot be applied. Of the remaining 27 targets

²Version 3.4 for all but 2M00274534-0806046 which used Version 4.2

with $\text{SpT} \geq \text{M5}$, 17 candidates (64%) exhibited signs of youth, i.e. intermediate (INT-G) or very low gravity (VL-G). These targets were then observed with high-resolution optical spectroscopy as described below to measure $\text{H}\alpha$, Li and radial velocities (RV). Other than three with ambiguous designations, all were confirmed as BPMG members. Our SpeX near-IR spectra are displayed in Figure 2.

4. Membership Confirmation with Optical High-Resolution Spectra

High-resolution spectra provide the RV necessary to calculate the space velocity (UVW), using the distance and proper motions, and thus to kinematically match the target to the moving group. With kinematic false membership rates of $\sim 50\%$ cumulatively for all YMGs and 6% for the BPMG (e.g. Pompéia et al. 2011; Shkolnik et al. 2012), both kinematics and independent spectral youth indicators are necessary to confirm a target as a bona fide YMG member. By combining all these data, we then designate each candidate in Table 3 with a membership status of ‘N’ for a non-member when the kinematics or youth indicators conflict with membership, ‘Y’ for confirmed members, and ‘Y?’ for likely members, but whose radial velocities differ from the predicted values due to binarity in the system. Our assessment procedure is summarized in Figure 3. In this study, we used the kinematic distance derived by assuming a candidate is a group member and thus report the UVWs only for those which we assess to indeed be members.

We acquired high-resolution optical spectra of our BPMG candidates, excluding those with IR spectra indicating field surface gravities, over seven nights with Magellan Inamori Kyocera Echelle (MIKE) optical echelle spectrograph on the Clay telescope at Magellan Observatory and two nights with Keck’s High Resolution Echelle Spectrometer (HIRES). (See Tables 1 and 3.)

The MIKE data were collected with the 0.5'' slit with a corresponding spectral resolution of $\approx 35,000$ across the 4900–10000 Å range of the red chip. The data were reduced using the facility pipeline (Kelson 2003).³ Each stellar exposure was bias-subtracted and flat-fielded. After extraction of each order, the one-dimensional spectra were wavelength calibrated with a ThAr arc lamp, which was taken after every stellar exposure to limit temperature differences and spectral drifts between the lamp and target exposures. To correct for any remaining instrumental drifts, we used the telluric O₂ A band (7620–7660 Å) to align the MIKE spectra to < 40 m/s. We then corrected for the heliocentric motion of the Earth. The final spectra are of moderate S/N (≈ 35 per pixel at 7000 Å).

³<http://code.obs.carnegiescience.edu/mike>

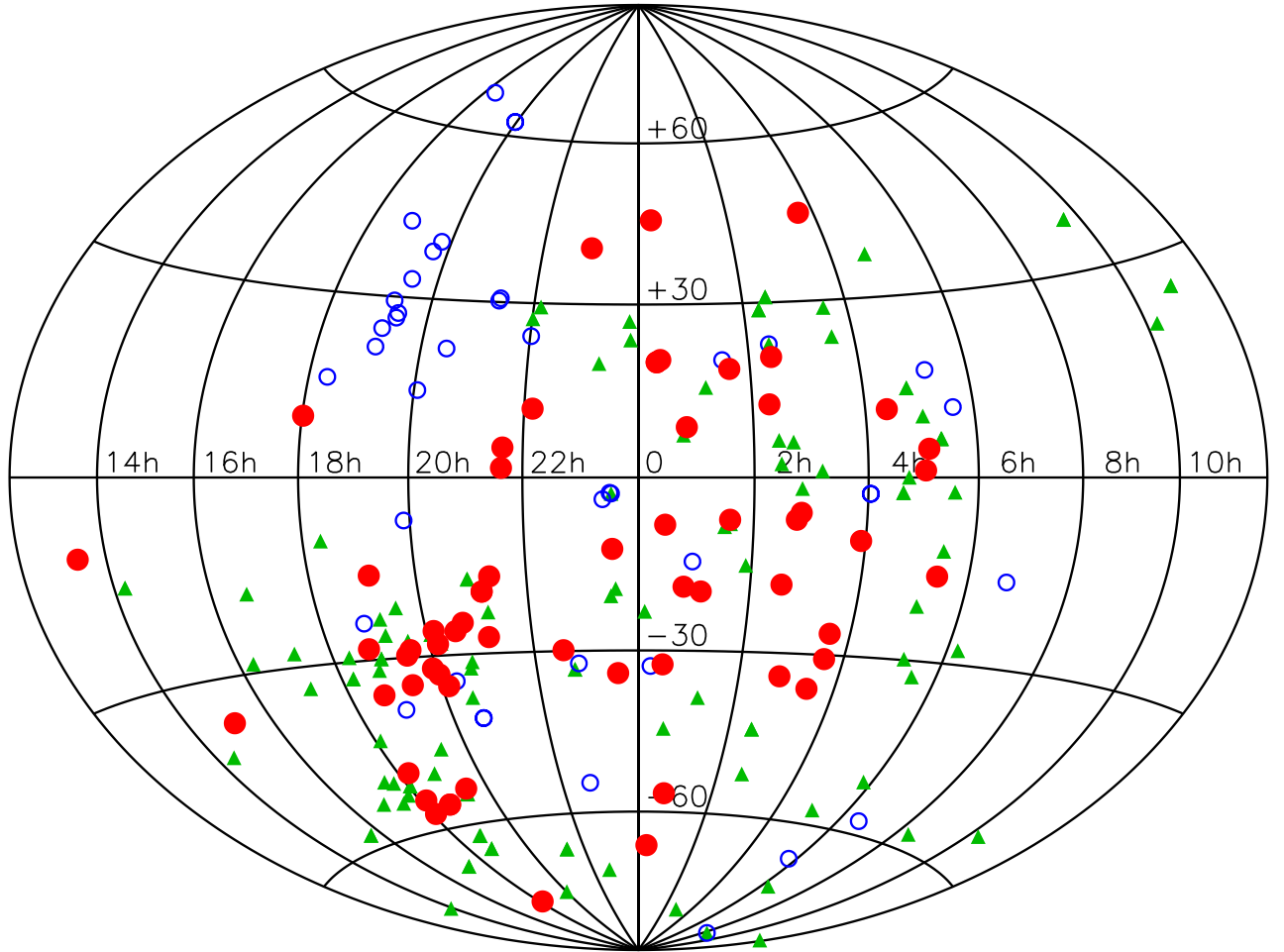


Fig. 1.— Positions of our candidate BPMG members on the sky shown in Aitoff projection. Candidates confirmed to be bona fide members (with both ‘Y’ and ‘Y?’ membership assessment in Table 3) are shown with red filled circles, while interloper field stars are shown with blue open circles. Known members from the literature (Appendix) are shown with filled green triangles.

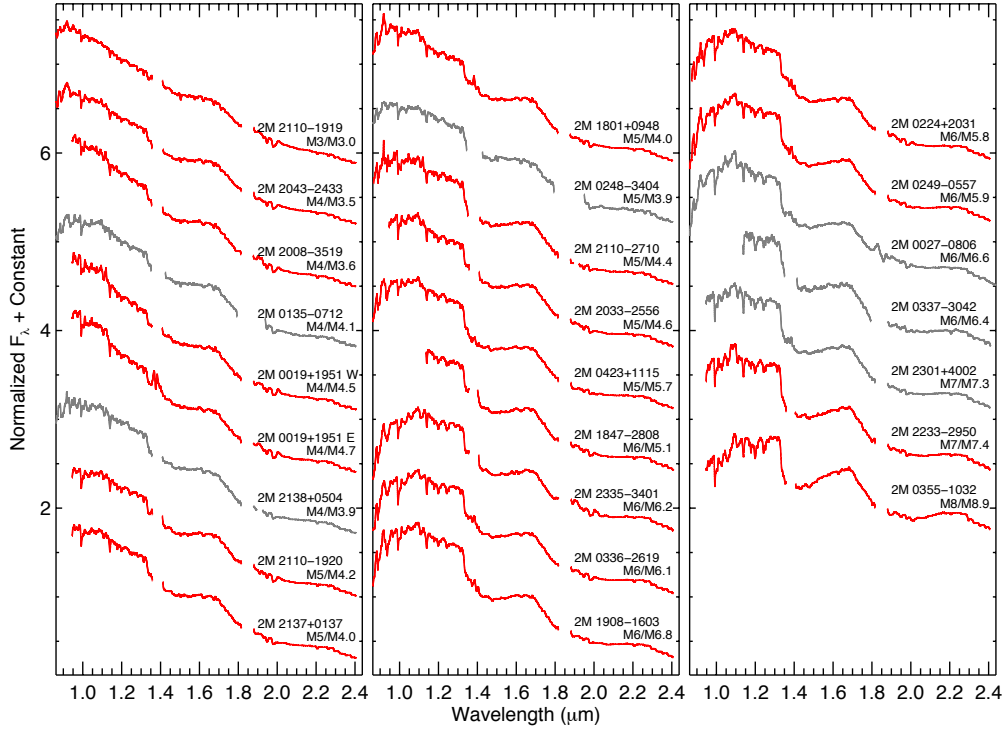


Fig. 2.— SpeX spectra of BPMG members. All spectra have been smoothed to a resolution, $\lambda/\Delta\lambda = 200$. Objects that we confirm as members of BPMG are plotted in red. Likely members (with a ‘Y?’ designation in Table 3), are plotted in grey. For each object the near-IR spectral type and SED spectral type are labeled ($\text{SpT}_{\text{NIR}}/\text{SpT}_{\text{SED}}$), and agree to within one subclass.

We used the 0.861" slit with HIRES to give a spectral resolution of \approx 58,000. The detector is a mosaic of three 2048×4096 $15\text{-}\mu\text{m}$ pixel CCDs spanning 4900–9300 Å and designated as the blue, green, and red chip. We used the GG475 filter with the red cross-disperser to maximize the throughput near the peak of an M dwarf spectral energy distribution. The HIRES data were reduced using the facility pipeline MAKEE⁴ written by T. Barlow. The MAKEE pipeline performs bias subtraction, flat-field correction, spectral extraction, wavelength calibration using the ThAr spectra, and a heliocentric velocity correction.

On each night, we observed RV standards with spectral types spanning those of our BPMG candidates. The standards were taken from Nidever et al. (2002), with updated RVs if available from Chubak et al. (2012). Each night, spectra were also taken of an A0V standard star for telluric line correction. Spectroscopically derived SpTs (SpT_{spec}) are listed in Table 3. For the late-type members we list the near-IR SpT. Optical SpTs were done with either TiO band indices or spectral line fitting following Shkolnik et al. (2009) and Kraus et al. (2014), respectively. In some cases due to poor continuum fitting, we include literature spectroscopic spectral types.

4.1. Radial Velocities for Kinematic Matches to the BPMG

Since our targets are relatively red, we limited our RV measurements to the reddest orders where the S/N is the highest. We cross-correlated each order between 7000 and 9000 Å (excluding those orders with strong telluric absorption) using the IRAF routine FXCOR (Fitzpatrick 1993). We measured the RVs from the Gaussian peak fitted to the cross-correlation function of each order and adopted the average RV of all orders with their standard deviation as the measurement uncertainty. The MIKE and HIRES data provide RV measurements to better than 1 km/s in almost all cases.

The target RVs are listed in Table 3 along with the difference in measured and predicted RV, assuming the star is a BPMG kinematic match: $\Delta\text{RV} = \text{RV}_{obs} - \text{RV}_{kin}$. With an RV dispersion of known BPMG members of 1.8 km/s (Mamajek & Bell 2014), we designate a star to be a kinematic match if $|\Delta\text{RV}| < 5.4$ km/s, a 3σ deviation from a perfect match (Figure 4).

The high resolution of the optical spectra also allow for the identification of double- or triple-lined spectroscopic binaries (SBs). Ten of our targets are SBs, consisting of seven SB2s, two SB3s, and one SB1s (2MASS J02485260-3404246, $\text{SpT}_{SED}=\text{M3.9}$) which appears

⁴http://www.astro.caltech.edu/~tb/ipac_staff/tab/makee/index.html

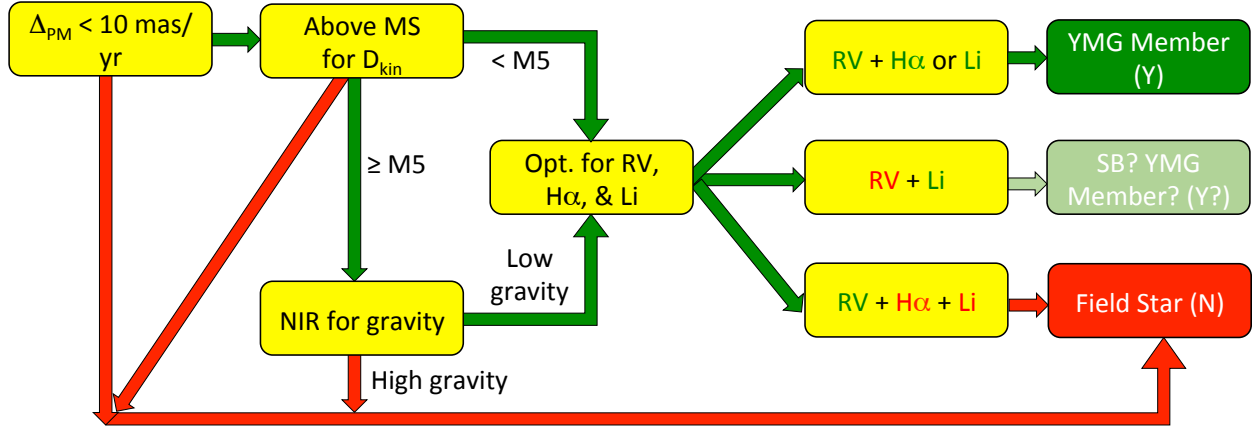


Fig. 3.— Flowchart for prescribing our young moving group selection process where red connectors and font denote “No” and green connectors and font denote “Yes”. An RV match is made when $|\Delta\text{RV}|$, the absolute difference between the kinematically predicted RV and the measured RV, is $< 5.4 \text{ km/s}$. An H α match implies that the EW of the emission lies above the empirically determined limit derived by Stauffer et al. (1997) for young ($\approx 50 \text{ Myr}$) clusters. The final status designations of ‘Y’, ‘Y?’ and ‘N’ are listed for each candidate in Table 3.

to be RV variable when compared to literature RV values. Of the 10 SBs we identified (Table 3),⁵ eight have systemic RVs consistent with BPMG members.

4.2. H α Emission and Lithium Absorption as Youth Indicators

Nearly all young stars with SpT \geq M0 exhibit Balmer emission, most notably H α . Stauffer et al. (1997) demonstrated a clear demarcation between older M dwarfs and those younger than the \approx 50 Myr old clusters, IC 2602 (Dobbie et al. 2010) and IC 2391 (Barrado y Navascués et al. 2004). Exceptionally strong H α emission also can indicate that a young star still hosts a gas-rich protoplanetary disk, where accreting gas is falling along magnetic field lines from the circumstellar disk onto the star (e.g. Barrado y Navascués & Martín 2003). None of our targets showed signs of accretion, which is not unexpected at the BPMG’s age.

We apply the Stauffer et al. (1997) H α criterion to our sample to identify those with emission levels consistent with stars younger than \approx 50 Myr. The H α equivalent widths (EW) for our sample are plotted in Figure 5 (left) identifying those stars we confirmed as BPMG members (as prescribed in Section 5 and Figure 3). Those cases with strong H α emission, but we do not identify as BPMG members, have $|\Delta\text{RV}| > 5.4 \text{ km/s}$.

Lithium (Li) absorption at 6708 Å is another spectroscopic age indicator in the optical spectrum of pre-main sequence stars. Stars with M0 < SpT < M5 require 20–100 Myr to deplete their primordial lithium (Chabrier et al. 1996), with depletion time scales increasing for later SpTs. The earlier SpTs therefore allow for tighter age constraints. For objects with SpT \geq M6, the detection of lithium sets an upper limit of \approx 100 Myr on the star’s age (Chabrier et al. 1996; Stauffer et al. 1998). We use the detection of lithium to be a solid indication of youth. However, the lack of lithium absorption in the spectra of early Ms is not confirmation of old age because the depletion timescales are short, providing an age limit comparable to the age of the BPMG. We measured lithium EWs or set limits⁶ for all of our targets for which we acquired optical spectra (Figure 5, right). An analysis of the lithium depletion boundary and corresponding age for the BPMG is presented in Section 5.1.

⁵The fraction of 10% SBs identified in this sample is lower than the 16% found by Shkolnik et al. (2010), because the earlier study was pre-selected for high X-ray activity, biasing the sample towards tightly-orbiting, tidally spun-up SBs.

⁶The lithium abundances have not been corrected for possible contamination with the Fe I line at 6707.44 Å. Uncertainties in the setting of continuum levels prior to measurement induce EW errors of about 10–20 mÅ with a dependence on the S/N in the region. We therefore consider our 2σ detection limit to be 0.05 Å.

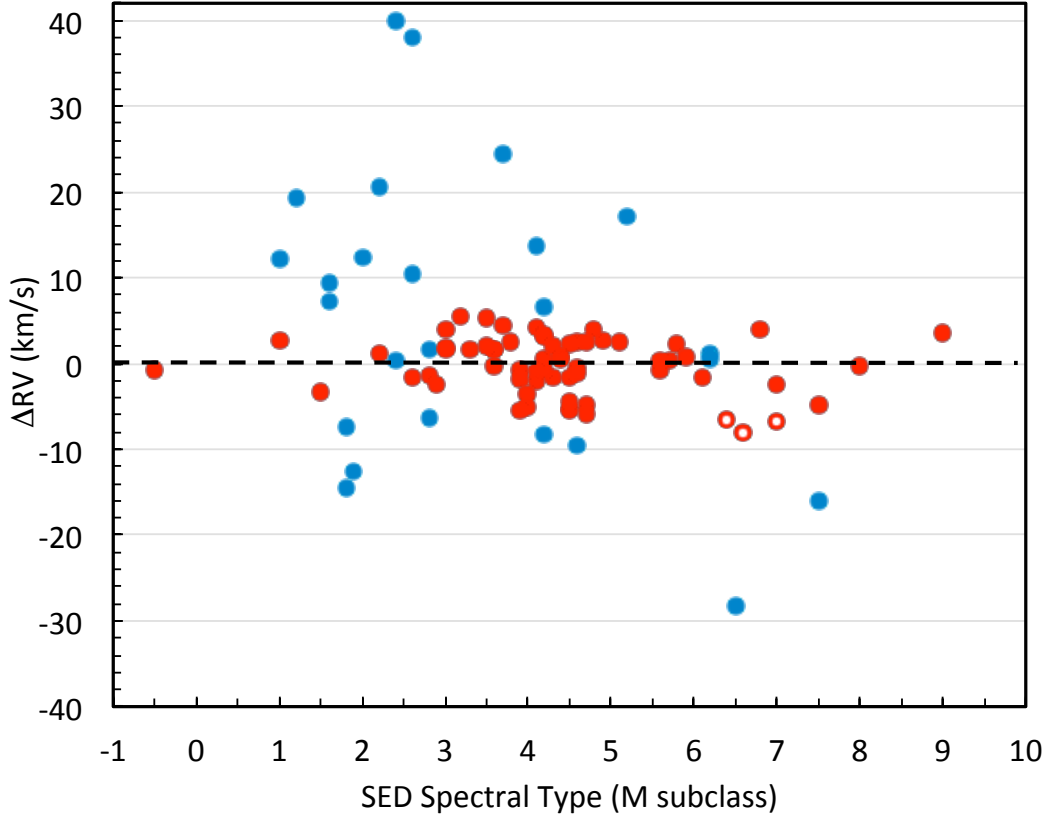


Fig. 4.— RV difference ($\Delta RV = RV_{obs} - RV_{kin}$) for our targets observed with high resolution optical spectroscopy as a function of spectral type. We use the SpT_{SED} for all targets with $SpT_{SED} < M7$. For objects $> M7$, we plot the spectroscopically determined SpT listed in Table 3. As in Figure 1, members are denoted with filled red circles and nonmembers with blue circles. Three possible members (with ‘Y?’ designation shown as open red circles) have slightly discrepant RVs ($|\Delta RV| > 5.4$ km/s), which may be due to unresolved binarity (SB1) but are confirmed to be young by the presence of Li absorption. These may also be young field interlopers.

Three of our candidates have strong H α in emission and Li absorption yet do not have RVs consistent with BPMG membership. We have designated these as possible members (with ‘Y?’) they may be SB1s where an unseen companion is causing the RV deviation. Alternatively, these are young field interlopers into our sample.

5. Summary of Confirmed BPMG Members

The methodology of the ACRONYM of the BPMG is summarized in Figure 3, which traces the prescription of our candidate selection and confirmation. We combine proper motion limits, suggestion of pre-main-sequence luminosity through photometric distance constraints, spectroscopic youth indicators such as low gravity, Li and H α , and RVs for kinematic matching.

Of our 104 BPMG candidates with follow-up IR and/or optical spectroscopy, we confirmed 66 member systems, recovering 25 previously reported members and identifying 41 new ones. Nineteen of the 66 members have spectroscopic or visual companions. All of our candidates with their final membership status are listed in Table 3. Fourteen of the 66 members have ‘Y?’ status. Ten of the candidates are SBs with system RVs consistent with the BPMG, strong H α emission, with two of these with strong Li absorption confirming youth. Eight of the SBs have inconclusive Li observations, but to avoid biasing the sample against SBs, we designate these with no Li information as ‘Y?’ . These systems should be followed up for full orbital solutions and/or parallaxes to better understand their membership status.

Our confirmation yield for BPMG systems is 66 of 104 candidates (63%), a little lower than the 67% confirmation rate we achieved in our Tuc-Hor study (Kraus et al. 2014). The slightly lower yield results from the extension of our search to positions further north than known BPMG members. Though this extension decreased our spectroscopic yield, it allowed us to determine the northern boundary of the BPMG (Figure 1).

The space velocities (UVW) and positions (XYZ) of confirmed members were calculated using the positions, RVs, proper motions, and kinematic distances. They are compared to the YMGs in Figure 6 and are listed in Table 3. The few outliers in these figures are the known or suspected SBs. Of the kinematic matches to the BPMG, only two are clearly not members, implying a 3% false-membership rate based on kinematics alone. This number is slightly less than that calculated by Shkolnik et al. (2012), who measured the UVWs of all the nearby old M dwarfs and found that 6% have kinematic matches to BPMG, but are clearly old. Our process for photometrically selecting pre-main sequence stars improves our ability to use kinematics to identify new candidate members.

To present the new mass function for the BPMG, we converted the SpT_{SED} for each target at an assumed age of 23 Myr to mass using the SpT–T_{eff} relation from Herczeg & Hillenbrand (2014) for SpTs of F5 and later and from Pecaut & Mamajek (2013) for stars earlier than F5. We then used the mass–T_{eff} relation from Baraffe et al. (2015) for stars with masses $\leq 1.4 M_{\odot}$, and the latest PARSEC models of Chen et al. (2015) for masses $> 1.4 M_{\odot}$.

In Figure 7 we compare the mass histogram for the BPMG before and after our confirmation of the new low-mass members. The new additions add 1, 2, 7, 17, and 10 objects respectively, in the lowest five mass bins. There are also 14 literature substellar objects, to which we add four more, for which we did not attempt to estimate the masses as they have SpTs later than M7 and the models for these have not yet been empirically calibrated.

5.1. Lithium Depletion and the Age of BPMG

Low-mass stars are gradually depleted of lithium as convection carries it deep into the stellar interior, where fusion converts it to helium. Lithium burning proceeds most rapidly for early-M stars (e.g., Figure 5, right), while stars of higher and lower mass burn lithium at correspondingly slower rates. This transition from lithium-rich to lithium-depleted is particularly rapid at the lower end of the depleted range, leading to a narrow “lithium depletion boundary” (LDB) that serves as a sensitive probe of age. The BPMG is one of the youngest nearby moving groups for which lithium depletion of early M dwarfs has been observed (e.g., Mentuch et al. 2008), leading to a lithium depletion age of $\tau = 24 \pm 4$ Myr (Binks & Jeffries 2016). The paucity of known M3–M5 members of BPMG has led to uncertainty in the location and width of the LDB, and hence the moving group’s age, but our newly identified BPMG members now densely sample this mass range.

In Figure 8, we plot the SpT_{SED}, absolute M_K magnitude, and lithium equivalent width of all of the K7–M6 members of the BPMG, as projected onto the three corresponding two-dimensional planes. The BPMG members without lithium are clearly clustered among the M1–M4 stars, with most $\leq M0$ and $\geq M4$ stars bearing at least some lithium. To provide context for the pattern of lithium depletion, we also show the isochronal tracks of Baraffe et al. (2015) in each plane, spanning ages of 15–50 Myr. We converted the isochrones into observational space by adopting their estimate of M_K , applying the SpT–T_{eff} temperature scale of Herczeg & Hillenbrand (2014), and applying the A_{Li} -EW[Li] curves of growth of Palla et al. (2007).

Our results clearly demonstrate the tension between theory and observations for age

determinations of young stars. In the HR diagram, nearly all sample members fall above the 15 Myr isochrone, implying a very young age of $\tau \sim 10$ Myr. However, the cluster sequence in M_K vs $EW[Li]$ implies an older age of $\tau \sim 25$ Myr, and the corresponding sequence in SpT_{SED} vs $EW[Li]$ implies an even older age of $\tau \gtrsim 50$ Myr. HR diagram ages are now broadly accepted to underestimate the true age of stars (e.g., Naylor 2009; Pecaut et al. 2012), most likely due to theoretical overestimation of T_{eff} for a given mass (e.g., Kraus et al. 2015). However, theory and observations seem to broadly agree on the relation between luminosity and mass for M stars at 10–50 Myr (Kraus et al. 2015; Montet et al. 2015; Rizzuto et al. 2016; Nielsen et al. 2016). The model-derived ages in our three observational planes are consistent with these patterns, so we hereafter refine our analysis to the ($EW[Li], M_K$) plane of Figure 8.

The observed sequence broadly agrees with the results of Binks & Jeffries (2016), who estimated the LDB age to be $\tau = 21 \pm 4$ Myr from the models of Baraffe et al. (2015) or $\tau = 24 \pm 4$ Myr from the magnetized models of Feiden (2016). Most of our observed lithium-bearing stars do indeed fall between the 20 and 25 Myr isochrones. However, Binks & Jeffries (2016) identified the LDB primarily via a discrete gap between the lithium-bearing and lithium-depleted members, while our more dense sequence also demonstrates for the first time that there is a finite width in SpT to the LDB. There is no clear gap in luminosity where there are no members with lithium, while lithium-depleted members extend as faint as $M_K = 6.6$. If we isolate the analysis to $\geq M2$ stars and identify the boundary to be the M_K where there are an equal number of lithium-depleted and lithium-rich members, then we find a boundary location of $M_K = 5.6$ mag, with 8 stars in each group. We find that 68% of the interlopers fall in the range of $5.2 < M_K < 6.0$ mag, so the corresponding uncertainty is ± 0.4 mag. The corresponding age from the Baraffe et al. (2015) models is $\tau = 22 \pm 6$ Myr.

Unresolved binarity could explain some extension of the lithium-bearing population upward, but it is difficult to explain the faintness of some lithium-depleted members; even the faintest lithium-depleted member (2MASS J03255277-3601161) shows excellent agreement with BPMG membership in all other aspects. The observations could indicate a genuine age spread, as has been suggested for AB Dor (López-Santiago et al. 2006) and for Taurus-Auriga/32 Ori (Kraus et al. 2017). However, it also might result from variations in lithium burning rates due to other stellar parameters. Lithium abundances have long been known to correlate with rotation for more massive stars (e.g., Soderblom et al. 1993), including in the BPMG (Messina et al. 2016), and substantial variations in lithium abundance have also been seen in populations both younger (Upper Sco; Rizzuto et al. 2015) and older (Pleiades; Somers & Stassun 2017). Convective mixing could be correlated with rotation at varying levels of subtlety, from direct impact on the convective mixing length (Bouvier 2008), to magnetic activity suppressing convection (Chabrier et al. 2007; Feiden 2016), or even more

subtly due to delayed rise in the core temperature (Baraffe & Chabrier 2010; Somers & Pinsonneault 2014). There is no straightforward way to disentangle these effects until purely geometric ages from astrometric tracebacks become feasible. However, our measured width for the LDB ($M_K = 5.6 \pm 0.4$ mag) is three times broader than the corresponding boundary we measured in Tuc-Hor ($M_K = 7.12 \pm 0.16$) via identical techniques. Either the astrophysics broadening the sequence change between 20 Myr and 40 Myr, or the BPMG may indeed have a substantially larger age spread than Tuc-Hor.

Finally, we find two outliers for which their membership should be further inspected:

- 2MASS J03363144-2619578 (SpT_{SED}=M6.1; $M_K = 7.66$) appears to be partially depleted in lithium ($EW[Li] = 330$ mÅ), even though it should be undepleted according to both SpT and M_K . It also has been suggested as a candidate member of the Tuc-Hor moving group (Rodriguez et al. 2013; Gagné et al. 2015b), and its observed RV (= 16.7 ± 2.7 km/s) is only marginally more consistent with expectations for the BPMG (= 18.2 km/s) than for Tuc-Hor (= 13.8 km/s). The lithium abundance suggests that the older age of Tuc-Hor is more appropriate, but its membership will ultimately be confirmed by parallax. It should fall at $d = 25$ pc if in the BPMG or at $d = 50$ pc if in Tuc-Hor.
- 2MASS J02365171-5203036 (=GSC 08056-00482) was proposed by Zuckerman & Song (2004) to be an M3 member of Tuc-Hor, but Elliott et al. (2014) subsequently classified it as an M2 member of the BPMG, and Malo et al. (2014a) used their BANYAN formalism to estimate a most likely membership in Columba, albeit with a significant probability for BPMG and a small probability for Tuc-Hor. This star sits low on the cluster sequence for BPMG, but its high lithium abundance for its SpT ($EW[Li] = 380$ mÅ; Torres et al. 2006) would be inconsistent with Tuc-Hor or Columba membership for M2–M3 stars (e.g., Kraus et al. 2014), and is high even for the BPMG. Membership in the BPMG seems most likely, but a parallax would clarify the question of membership for this star.

6. Conclusion

In this paper we present the results from our efficient photometric+kinematic selection process, which identified 104 low-mass BPMG candidates. Follow-up infrared observations of the latest spectral types (SpT > M5) were collected with IRTF/SpeX to search for low gravity objects, an indication of youth. We observed the young ones of these, plus all the earlier SpT candidates with the high-resolution optical spectrographs at the Magellan and

Keck telescopes. These data provided the RVs needed to confirm or reject stars co-moving with the BPMG and youth indicators such as Li absorption and H α emission.

Prior to our work, there were 94 known member systems with primary masses less than $0.7 M_{\odot}$. We compiled the current census in the Appendix with which we were able to test the efficiency and false-membership assignments using our selection and confirmation criteria. The addition of 41 new systems from this work represents a 44% increase in low-mass BPMG membership and a new sample around which to look for directly-imaged planets. The four new BPMG members with SpTs $\geq M7$, and likely less than $0.07 M_{\odot}$, represents a 29% increase to the 14 already known. They are: 2MASS J00413538-5621127, 2MASS J03550477-1032415, 2MASS J22334687-2950101, and 2MASS J23010610+4002360. If the number of BPMG’s AFGK stars is complete, then the fraction of M stars in the BPMG is now 69% nearing the expected value of 75%. However, the new IMF for the BPMG clearly shows a deficit of $0.2\text{--}0.3 M_{\odot}$ stars by a factor of ~ 2 . We except that the AFGK census of the BPMG is *also* incomplete, probably due to biases of searches towards the nearest of stars. Future surveys for AFGK and M spectral type members should extend out to at least 100 pc for the BPMG.

7. Appendix: Members of BPMG From the Literature

To complement our search for new members, we compiled the most comprehensive list of the 146 objects that have been reported in the literature as likely members of the BPMG in Table 4. This list includes every object that has been asserted to be a member, as well as any probabilistic candidates that have $> 50\%$ membership probability (e.g., Malo et al. 2013). Past stars considered members that were later refuted by more data are not included (Binks & Jeffries 2016; Elliott et al. 2016; Liu et al. 2016.) We also exclude any purported members from traceback analyses (Ortega et al. 2002; Song et al. 2003; Makarov 2007) as recent revisions to the age of the BPMG cast doubt on tracebacks conducted with the previous (younger) age (Mamajek & Bell 2014). In compiling our census, we included every object that has a distinct entry in the 2MASS Point Source Catalog (Cutri et al. 2003), but did not include secondary components of close multiple systems. The effective angular separation cutoff is $\approx 4\text{--}5''$. We list the previously reported members in Table 4 along with all available data used for membership assessments: spectral types, proper motions, RVs, H α EWs, Li EWs, and surface gravity assessments. We also compiled parallaxes for 77 of the objects in the literature census. Parallaxes are not currently available for any sources in our own survey. For easier use of the complete census, we appended the new BPMG members from this work to the bottom of Table 4.

We subjected the 113 published members with K and M spectral types to the same tests described in Sections 3–5 as a test of the methodology. The results of those tests are summarized below:

- 88 have membership designations of ‘Y’ (77.9%).
- 17 have ‘Y?’ (15.0%) because the star’s $RV = ?$ or ‘N’, but it has $H\alpha = ‘Y’$, $Li = ‘Y’$ and/or has been shown to have low surface gravity.
- 6 have membership=‘N’ (5.3%):
 - ◊ 4 of these have $RV = ‘Y’$ but membership=‘N’ because $H\alpha = ‘N’$ and $Li = ?$. These cases may be the few relatively *inactive* young stars that may exist, or are not in fact members with kinematics coincident with the BPMG.
 - ◊ 2 have $RV = ?$, $Li = ?$, $H\alpha = ?$ and field gravities from Gagné et al. (2015b) and are probably not BPMG members.
- 1 has membership=? (0.9%) because it has no RV, $H\alpha$, or Li information, and is reported to have low surface gravity.

Assuming all the literature-reported members in Table 4 are indeed members, below are fractions that do not pass each test, representing a possible false-negative rate for each age diagnostic:⁷

- 7 of 100 (7.0%) with published RV do not have velocities consistent with membership.
- 4 of 96 (4.2%) with measured $H\alpha$ have lower than expected emission for young stars.
- 2 of 12 (17%) with reported gravity classification have field level gravity and thus likely are not young.

In conclusion, we propose that these false-negative rates be considered when confirming new members, but caution should be applied to not use these in a circular fashion to increase our tolerance of each age diagnostic.

E.S. thanks J. Teske for useful discussions and appreciates support from the HST grant HST-AR-13911.002-A and NASA/Habitable Worlds grant NNX16AB62G. K.A. acknowledges support by a NASA Keck PI Data Award (#1496879), administered by the NASA

⁷Twenty-six of 74 (35.1%) stars have no measurable Li absorption, but this is not an indication of old age for BPMG members (Figure 5).

Exoplanet Science Institute. We also thank Dr. Eric Mamajek for a speedy and helpful referee’s report. This research has made use of the VizieR catalogue access tool, CDS, Strasbourg, France (Ochsenbein et al. 2000) and the Mikulski Archive for Space Telescopes (MAST). STScI is operated by the Association of Universities for Research in Astronomy, Inc., under NASA contract NAS5-26555. Support for MAST for non-HST data is provided by the NASA Office of Space Science via grant NNX13AC07G and by other grants and contracts.

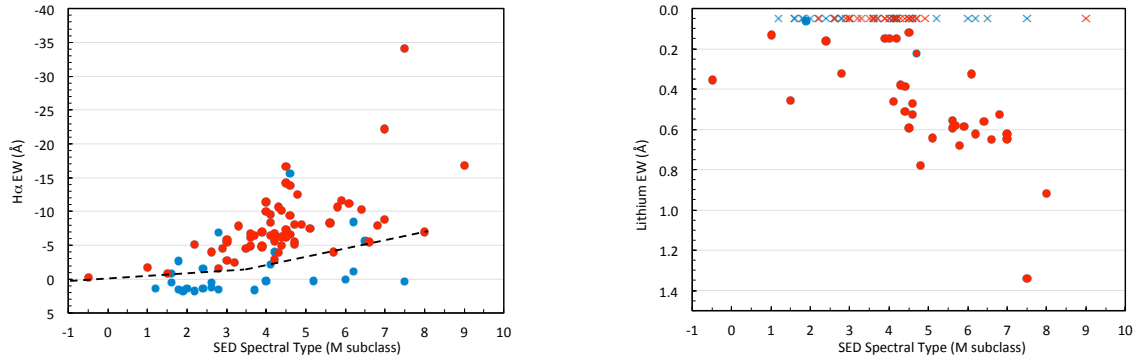


Fig. 5.— Sample distribution of H α emission (left) and lithium absorption (right) equivalent widths (EW). We use the SpT_{SED} for all targets with SpT_{SED} < M7. For objects > M7, we plot the spectroscopically determined SpT listed in Table 3. The confirmed members are shown in red and the non-members in blue. The dashed line in the left plot represents the lower bound for H α emission determined empirically by Stauffer et al. (1997) from young (\approx 50 Myr) clusters IC 2602 and IC 2391. Those cases with strong H α emission but we do not identify as BPMG members have $|\Delta RV| > 5.4$ km/s. An ‘x’ in the right plot represents an upper limit of 0.05 Å for lithium EW. An analysis of the lithium depletion boundary and corresponding age for the BPMG is presented in Section 5.1.

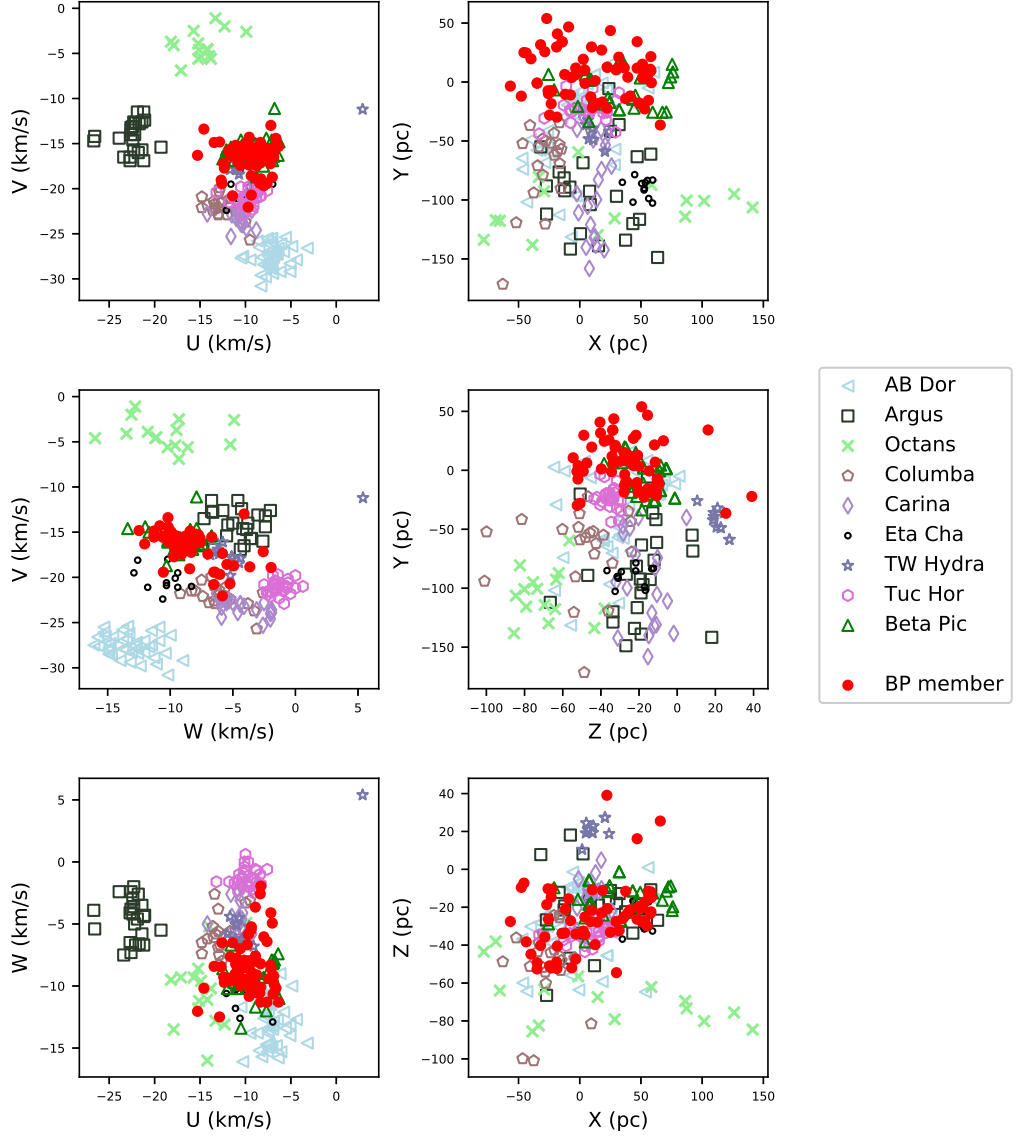


Fig. 6.— UVW and XYZ of known members of nine YMGs, including the new BPMG members reported in this work (red circles). The few outliers in U,W plot in the bottom left corner have ‘Y?’ based on known binarity, no lithium detection, or large RV uncertainty. The other YMG members are from Torres et al. (2008).

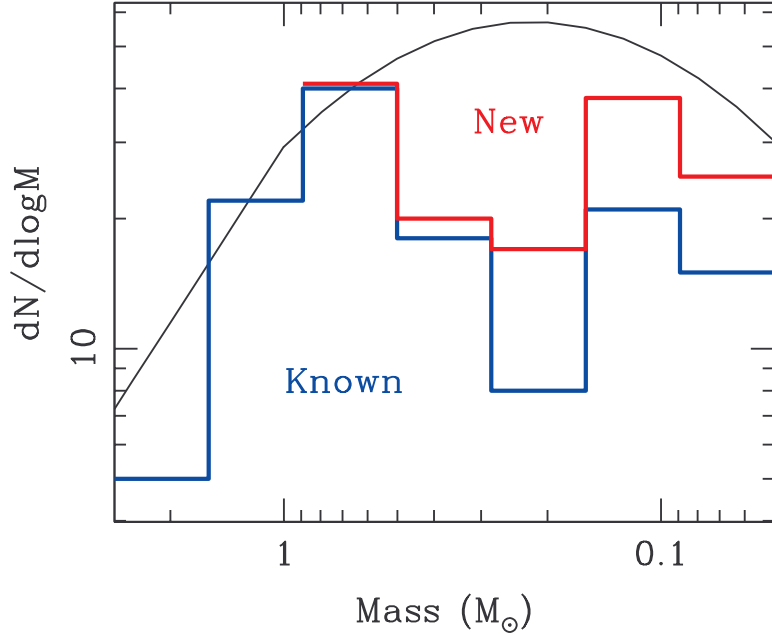


Fig. 7.— Mass histogram of BPMG member systems. The previously published members are shown in blue with the addition of those found in this study shown in red. The new additions add 1, 2, 7, 17, and 10 objects, respectively, in the lowest five bins. These increase the number of known M stars in the BPMG by 46% from 80 to 117. The black line shows the Salpeter+Chabrier IMF normalized to the most populated mass bin, indicating that there are a significant number of M stars remaining to be discovered. There are also 14 literature substellar objects not shown on this mass scale to which we add four more. We did not attempt to estimate the masses of those targets as they have SpTs later than M7 and the models for these have not yet been empirically calibrated.

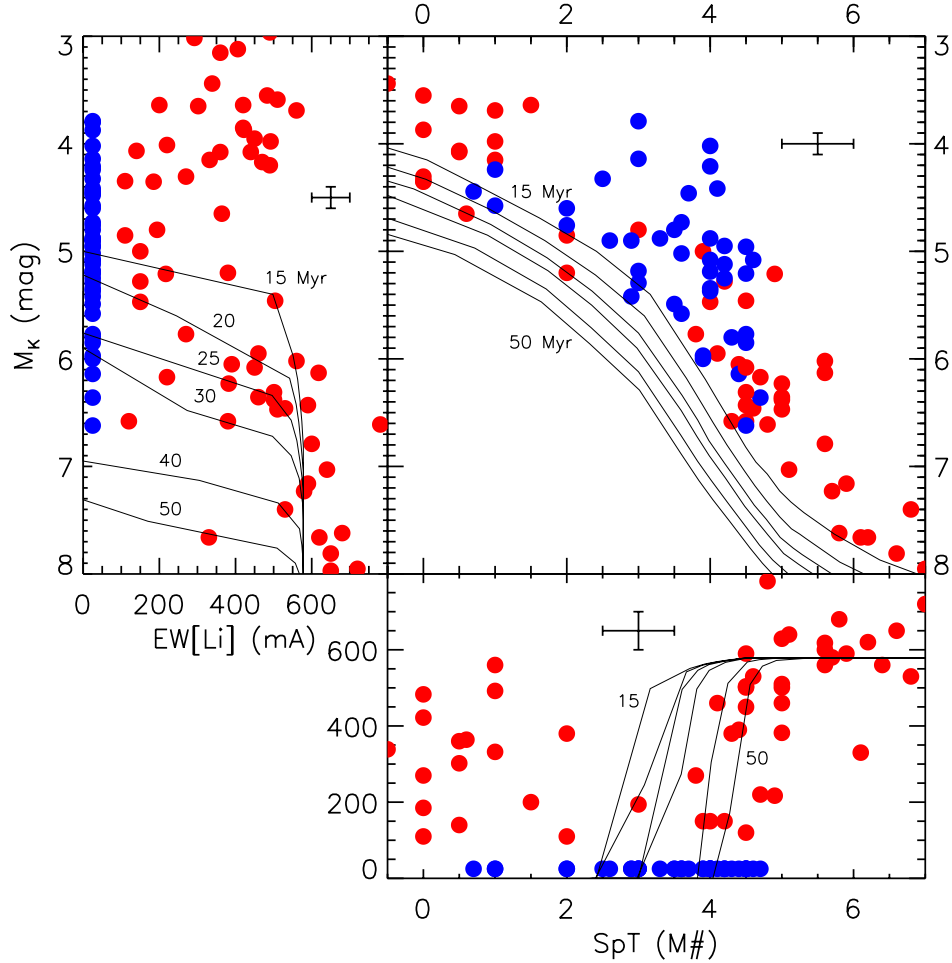


Fig. 8.— SpT_{SED} , absolute M_K magnitude, and lithium equivalent width of all of the K7–M6 members of the BPMG, as projected onto the three corresponding two-dimensional planes. The BPMG members without lithium (blue) are clearly clustered among the M1–M4 stars, with most $\leq M0$ and $\geq M4$ stars bearing at least some lithium (red). Representative error bars are shown on each plot. The isochronal tracks of Baraffe et al. (2015) are shown in each plane, spanning ages of 15–50 Myr. We converted the isochrones into observational space by adopting their estimate of M_K , applying the $SpT-T_{eff}$ temperature scale of Herczeg & Hillenbrand (2014), and applying the A_{Li} - $EW[Li]$ curves of growth of Palla et al. (2007).

Table 1. Selection Criteria and Observations of Candidate BPMG Members

2MASS J	R _{USNOB} (mag)	K _s (mag)	μ (mas/yr)	SpT _{SED}	m _{bol} (mag)	D _{Mplot} (mag)	$\Delta_P M$ (mas/yr)	D _{Mkin} (mag)	IR Spec. ^a	Opt. Spec.	UT date (yyymmdd)
00140580-3245599	18.86	12.03	(73,-46.3) ± 9.1	M7.7 ± 0.2	15.02 ± 0.02	2.02 ± 0.07	10.2	3.4	SXD	-	-
00164976+4515417	14.68	9.85	(62.5,-22.1) ± 3.5	M4.5 ± 0.3	12.61 ± 0.03	2.14 ± 0.25	9.6	4.0	-	Keck/HIRES	20120710
00172353-6645124	11.51	7.70	(104.3,-13.5) ± 1.0	M2.6 ± 0.4	10.31 ± 0.02	1.48 ± 0.24	2.4	2.8	-	Magellan/MIKE	20101229
00193331+1951050	14.39	10.08	(72.2,-49.7) ± 3.5	M4.5 ± 0.1	12.82 ± 0.02	2.36 ± 0.10	2.9	3.5	SXD	Magellan/MIKE	20101231
00194303+1951117	14.19	9.86	(70.6,-50.9) ± 3.5	M4.7 ± 0.1	12.64 ± 0.02	1.96 ± 0.10	4.9	3.5	SXD	Magellan/MIKE	20101231
00233468+2014282	9.97	7.34	(61.4,-38.3) ± 1.9	K7.6 ± 0.2	9.65 ± 0.04	2.34 ± 0.11	1.5	3.9	-	Keck/HIRES	20120710
00274334-0806046	16.46	10.61	(97.3,-66.9) ± 3.3	M6.5 ± 0.1	13.55 ± 0.02	1.10 ± 0.06	6.6	2.8	SXD	Keck/HIRES	20120710
00281433-3227556	13.97	9.28	(108.0,-42.6) ± 2.9	M4.3 ± 0.4	12.01 ± 0.04	1.76 ± 0.34	5.7	2.7	-	Keck/HIRES	20120710
00413538-5621127	18.06	10.86	(109.4,-52.9) ± 17.9	M7.9 ± 0.1	13.93 ± 0.02	0.84 ± 0.05	33.6	2.5	-	Magellan/MIKE	20101231
00482667-1847204	14.84	9.86	(74.9,-44.7) ± 2.3	M4.6 ± 0.2	12.64 ± 0.02	2.07 ± 0.20	4.3	3.4	-	Magellan/MIKE	20101231
00501752+0837341	13.44	8.90	(63.9,-34.5) ± 2.8	M3.9 ± 0.1	11.57 ± 0.02	1.74 ± 0.10	7.6	3.9	-	Magellan/MIKE	20101230
00570256-1425174	17.05	11.77	(57.6,-36.5) ± 4.6	M5.8 ± 0.3	14.63 ± 0.02	2.78 ± 0.30	3.5	3.9	SXD	-	-
01071194-1935359	11.11	7.25	(63.1,-39.8) ± 1.2	M2.8 ± 0.3	9.87 ± 0.02	0.91 ± 0.19	6.8	3.6	-	Magellan/MIKE	20101230
01303534+2008393	14.92	10.19	(56,-43.9) ± 5.2	M4.7 ± 0.3	12.98 ± 0.04	2.30 ± 0.24	1.9	3.9	-	Keck/HIRES	20120710
0137393-0712517	12.49	8.08	(97.7,-51.5) ± 4.2	M4.1 ± 0.1	11.79 ± 0.02	0.76 ± 0.10	8.9	2.8	SXD	Magellan/MIKE	20101230
01373940+1835332	9.93	6.72	(68.0,-47.0) ± 0.9	M1.5 ± 1.1	9.20 ± 0.09	0.99 ± 0.40	7.2	3.6	-	Magellan/MIKE	20101230
02175601+1225266	13.48	9.08	(51.2,-42.1) ± 4.6	M2.2 ± 0.2	11.69 ± 0.02	3.12 ± 0.09	4.2	4.0	-	Keck/HIRES	20120710
02232663+2244069	10.51	7.35	(99.0,-114.4) ± 2.0	M1.6 ± 0.9	9.88 ± 0.05	1.63 ± 0.43	8.5	2.2	-	Keck/HIRES	20120710
02241739+2031513	16.95	11.62	(52.7,-40.7) ± 3.2	M2.8 ± 0.2	14.45 ± 0.02	2.60 ± 0.18	9.5	4.0	SXD	Magellan/MIKE	20101230
02335084-1811525	13.04	9.22	(51.1,-23.5) ± 2.4	M2.9 ± 0.4	11.87 ± 0.03	2.85 ± 0.24	2.9	3.8	-	Keck/HIRES	20120710
02450826-0708120	14.37	9.95	(39.2,-38.3) ± 3.3	M4.1 ± 0.2	12.67 ± 0.01	2.64 ± 0.17	7.3	4.0	-	Magellan/MIKE	20101229
02485260-3404246	12.74	8.40	(89.0,-23.8) ± 1.4	M3.9 ± 0.4	11.09 ± 0.03	1.25 ± 0.30	7.7	2.4	SXD	Magellan/MIKE	20101229
02495639-0557352	16.81	11.06	(44.6,-35.0) ± 4.1	M5.9 ± 0.3	13.92 ± 0.02	1.97 ± 0.26	0.8	3.9	SXD	Magellan/MIKE	20101229
0325277-34601161	15.07	10.62	(34.7,-3.7) ± 3.1	M4.5 ± 0.1	13.36 ± 0.03	2.89 ± 0.09	1.6	4.0	-	Magellan/MIKE	20101229
03363144-2619578	9.76	7.97	(79.0,-25.5) ± 3.3	M6.1 ± 0.2	12.65 ± 0.02	0.53 ± 0.16	2.4	2.1	SXD	Magellan/MIKE	20101229
03370343-3042318	18.33	12.37	(31.7,-7.7) ± 4.7	M6.4 ± 0.2	15.24 ± 0.02	2.92 ± 0.13	1.2	4.0	SXD	Magellan/MIKE	20101229
03393700+4531160	13.22	9.09	(37.8,-74.7) ± 2.9	M3.5 ± 0.1	11.74 ± 0.02	2.23 ± 0.10	1.0	3.6	-	Keck/HIRES	20120710
0350477-1024245	19.08	11.98	(52.6,-38.4) ± 6.8	M8.9 ± 0.4	15.12 ± 0.02	1.72 ± 0.10	8.4	2.9	SXD	Keck/HIRES	20131024
04023239-0242335	11.47	7.55	(41.2,-38.9) ± 3.8	M2.6 ± 0.9	10.19 ± 0.05	1.36 ± 0.60	8.7	3.5	-	Magellan/MIKE	20101229
04023238-0242161	11.99	8.19	(36.0,-38.7) ± 5.4	M1.6 ± 1.2	10.74 ± 0.07	2.49 ± 0.69	4.7	3.6	-	Keck/HIRES	20131024
04232720+1115174	16.50	11.23	(26.3,-46.7) ± 4.3	M5.7 ± 0.4	14.07 ± 0.02	2.33 ± 0.40	4.2	4.0	SXD	Magellan/MIKE	20101229
05015665+0108429	12.08	7.68	(31.8,-90.4) ± 3.3	M3.6 ± 0.2	10.34 ± 0.02	0.75 ± 0.17	2.5	2.1	-	Magellan/MIKE	20101230
05061292+0439272	12.60	8.07	(32.7,-91.8) ± 3.5	M3.8 ± 0.2	10.75 ± 0.02	0.99 ± 0.12	7.4	2.3	-	Magellan/MIKE	20101230
05071137+1430013	14.69	9.66	(18.6,-72.1) ± 3.4	M4.9 ± 0.3	12.51 ± 0.03	1.61 ± 0.25	2.6	3.2	-	Magellan/MIKE	20101230
05115901+1728481	14.09	9.84	(13.0,-57.6) ± 4.4	M4.0 ± 0.3	12.53 ± 0.03	2.61 ± 0.26	2.1	3.8	-	Magellan/MIKE	20101230
05241914-1601153	12.55	7.81	(18.0,-35.4) ± 3.5	M4.9 ± 0.2	10.62 ± 0.02	-0.28 ± 0.21	5.2	2.6	-	Magellan/MIKE	20101229
05363384+1117487	11.38	7.41	(-38.6,-61.2) ± 3.2	M2.3 ± 0.4	10.07 ± 0.02	0.81 ± 0.30	8.5	3.5	-	Magellan/MIKE	20101230
05432597-6630096	-	10.86	(-12.4,-66.1) ± 11.0	M6.0 ± 0.2	13.77 ± 0.02	1.71 ± 0.19	15.7	2.9	-	Magellan/MIKE	20101230
06352229-5737349	10.25	7.15	(-17.6,-51.3) ± 0.9	M1.0 ± 0.2	9.66 ± 0.02	1.69 ± 0.07	2.2	2.8	-	Keck/HIRES	20120710
06451593-1622030	17.95	11.93	(-15.9,-24.7) ± 4.5	M6.5 ± 0.4	14.80 ± 0.03	2.42 ± 0.20	1.3	3.6	-	Magellan/MIKE	20101231
08173943-8243298	10.50	6.59	(-81.9,-102.6) ± 1.2	M3.0 ± 0.3	9.23 ± 0.04	0.14 ± 0.14	3.0	2.1	-	Magellan/MIKE	20101614
13215631-1052098	-	8.62	(-71.6,-49.8) ± 3.4	M4.2 ± 0.3	11.33 ± 0.04	1.2 ± 0.25	3.3	3.5	-	Magellan/MIKE	20101614
15063505-3632997	15.84	11.11	(-42.3,-38.2) ± 10.6	M4.8 ± 0.2	13.94 ± 0.02	3.14 ± 0.20	13.2	4.5	-	Keck/HIRES	20120710
18011345+0948379	13.66	9.37	(-4,-28.3) ± 3.1	M4.0 ± 0.3	12.10 ± 0.03	2.18 ± 0.26	7.1	3.9	SXD	Keck/HIRES	20120710
18055491-5704307	12.85	8.63	(-0.1,-72) ± 6.4	M3.6 ± 0.6	11.32 ± 0.04	1.74 ± 0.48	4.3	3.9	-	Magellan/MIKE	20120902
18090694-7613239	14.18	8.99	(11.2,-152.8) ± 3.0	M5.6 ± 0.5	11.81 ± 0.02	0.17 ± 0.46	1.1	2.2	-	Magellan/MIKE	20120902
18092970-5430532	14.32	9.12	(6.8,-103.7) ± 2.8	M5.6 ± 0.4	11.95 ± 0.03	0.31 ± 0.33	2.0	3.1	-	Keck/HIRES	20120710
18151564-4974742	12.22	8.04	(8.8,-71.5) ± 1.6	M3.0 ± 0.4	10.69 ± 0.02	1.60 ± 0.25	2.0	3.9	-	Magellan/MIKE	20110614
18211526+1610078	10.68	7.48	(10.9,-19.3) ± 3.5	M1.2 ± 0.4	10.04 ± 0.03	1.97 ± 0.15	3.0	3.9	-	Keck/HIRES	20120710
18224692+6723001	18.83	12.35	(10.7,-43.2) ± 6.7	M7.2 ± 0.2	15.33 ± 0.02	2.55 ± 0.09	1.8	3.8	SXD	-	-

Table 1—Continued

2MASS J	R _{USNOB} (mag)	K _s (mag)	μ (mas/yr)	SpT/SED	m _{bol} (mag)	D _{phot} (mag)	ΔP_M (mas/yr)	D _{Mken} (mag)	IR Spec. ^a	Opt. Spec.	UT date (yyyy-mm-dd)
18420483-5554126	14.47	9.85	(12.9,-74.0) ± 5.2	M4.4 ± 0.3	12.55 ± 0.03	2.21 ± 0.25	2.0	3.8	—	Magellan/MIKE	20110614
18420694-5554254	12.66	8.58	(11.2,-81.4) ± 4.0	M3.3 ± 0.4	11.26 ± 0.03	1.92 ± 0.31	4.5	3.7	—	Magellan/MIKE	20110614
18435838-35539096	14.38	10.33	(20.9,-65.9) ± 6.5	M4.5 ± 0.9	13.10 ± 0.06	2.63 ± 0.77	6.9	3.9	SXD	Keck/HIRES	20120710
18471351-2808555	15.94	10.83	(8.6,-69.0) ± 4.1	M5.1 ± 0.3	13.69 ± 0.02	2.57 ± 0.27	7.8	3.8	SXD	—	—
18504473-2353389	—	11.46	(9.7,-78.0) ± 16.9	M6.0 ± 0.8	14.31 ± 0.04	2.25 ± 0.69	10.6	3.4	SXD	Keck/HIRES	20120710
18505451+4259510	13.54	8.92	(44.4,-21.6) ± 3.4	M4.2 ± 0.3	11.65 ± 0.03	1.51 ± 0.25	8.0	2.1	—	Keck/HIRES	20120710
19033299-3847058	14.67	9.73	(33.3,-117.5) ± 2.3	M5.2 ± 0.3	12.59 ± 0.03	1.37 ± 0.25	0.3	2.7	SXD	Keck/HIRES	20120710
19082110+2129364	13.00	8.87	(16.2,-21.9) ± 4.3	M3.7 ± 0.4	11.55 ± 0.03	1.88 ± 0.28	8.2	3.8	SXD	Keck/HIRES	20120710
19082195-1603249	16.77	11.40	(20.6,-50.9) ± 3.6	M6.8 ± 0.1	14.19 ± 0.04	1.62 ± 0.10	1.1	4.0	SXD	Keck/HIRES	20120710
19103551+2436150	8.85	5.77	(18.3,-14.1) ± 1.0	M1.8 ± 0.2	8.36 ± 0.03	0.01 ± 0.06	3.8	4.0	—	Keck/HIRES	20120710
19153643+2920117	11.05	7.70	(29.5,-3.1) ± 16.2	M2.0 ± 0.2	10.29 ± 0.03	1.85 ± 0.15	4.4	3.4	—	Keck/HIRES	20120710
19234422+2629030	11.10	7.88	(37.8,-25.2) ± 4.3	M2.4 ± 0.2	10.49 ± 0.03	1.79 ± 0.15	9.7	2.8	—	Keck/HIRES	20120710
19242697+2716351	12.26	8.82	(24.7,-6.0) ± 3.2	M2.6 ± 0.4	11.46 ± 0.03	2.63 ± 0.21	2.6	4.0	—	Magellan/MIKE	20110614
19243494-3442392	13.27	8.78	(23.2,-72.1) ± 1.8	M4.6 ± 0.2	11.55 ± 0.04	0.98 ± 0.13	4.0	3.7	—	Magellan/MIKE	20110614
19260075-5331269	13.16	8.68	(34.1,-88.1) ± 2.0	M4.2 ± 0.3	11.43 ± 0.03	1.29 ± 0.24	3.0	3.4	—	Magellan/MIKE	20120902
19275844+3309439	10.47	7.34	(38.4,-1.4) ± 2.1	M1.9 ± 0.2	9.97 ± 0.03	1.58 ± 0.07	1.3	3.0	—	Keck/HIRES	20120710
1930396-29539322	13.61	9.25	(22.8,-59.4) ± 3.6	M4.2 ± 0.1	11.96 ± 0.02	1.83 ± 0.10	2.0	4.0	—	Keck/HIRES	20120710
19355395-2846343	—	12.71	(26.6,-58.9) ± 5.1	L1.0 ± 0.45 ^b	15.90 ± 0.03	2.09 ± 0.10	0.7	4.0	SXD ^c	Keck/HIRES	20131024
19410521+3806521	12.19	8.24	(31.8,-1.0) ± 3.3	M2.2 ± 0.4	10.86 ± 0.03	2.29 ± 0.22	2.5	3.7	—	Keck/HIRES	20120710
19472175+3954072	12.19	10.43	(26.9,-25.7) ± 17.5	M7.5 ± 0.3	13.51 ± 0.03	0.60 ± 0.11	21.2	3.9	SXD	Magellan/MIKE	20110615
19533169-07207001	14.97	9.93	(39.1,-43.9) ± 2.8	M5.0 ± 0.3	12.75 ± 0.02	1.74 ± 0.25	7.1	3.8	SXD	—	—
19560294-32207186	12.59	8.11	(32.6,-61.0) ± 1.5	M3.7 ± 0.4	10.82 ± 0.04	1.14 ± 0.31	0.6	3.9	—	Keck/HIRES	20120710
19571814+6242573	17.58	11.99	(38.1,-21.4) ± 3.8	M6.5 ± 0.9	14.88 ± 0.04	2.5 ± 0.74	4.0	4.0	SXD	—	—
19572094+6242559	19.38	12.56	(38.5,-24.2) ± 6.4	M7.3 ± 0.2	15.57 ± 0.02	2.74 ± 0.08	7.7	3.8	SXD	—	—
20013718-3313139	11.62	8.24	(27.1,-60.9) ± 2.2	M1.0 ± 0.3	10.75 ± 0.03	2.78 ± 0.10	5.3	4.0	—	Magellan/MIKE	20110614
20034245+1432215	10.77	7.26	(20.9,-39.3) ± 15.0	M2.8 ± 0.2	9.95 ± 0.03	0.60 ± 0.11	21.2	3.9	SXD	Keck/HIRES	20120710
20083784-2452556	14.94	10.07	(28.6,-60.4) ± 2.8	M4.7 ± 0.2	12.84 ± 0.02	1.74 ± 0.25	7.1	3.8	SXD	Keck/HIRES	20120710
20085368-3519486	12.71	8.32	(48.8,-80.1) ± 1.3	M3.6 ± 0.3	10.95 ± 0.02	1.36 ± 0.21	2.8	3.3	SXD	Keck/HIRES	20120710
20100002-2801410	12.16	7.73	(40.4,-62.7) ± 0.9	M4.1 ± 0.2	10.46 ± 0.04	1.43 ± 0.13	2.2	3.7	SXD	Magellan/MIKE	20110614
20200623-3433203	17.13	12.00	(36.1,-59.7) ± 7.2	M6.1 ± 0.7	13.88 ± 0.03	2.76 ± 0.68	1.6	3.9	SXD	—	—
20285054+2141119	13.46	9.13	(53.2,-31.4) ± 4.9	M4.1 ± 0.2	11.81 ± 0.03	1.79 ± 0.14	5.8	3.2	SXD	Magellan/MIKE	20110614
20333759-2556521	14.02	8.88	(51.8,-76.8) ± 1.5	M4.6 ± 0.1	11.65 ± 0.02	1.07 ± 0.10	3.5	3.3	SXD	Magellan/MIKE	20120902
20385687-4118285	15.95	10.74	(49.9,-52.7) ± 8.4	M6.2 ± 0.2	13.63 ± 0.03	1.44 ± 0.12	11.1	3.9	—	Keck/HIRES	20120710
20390476-4117390	14.23	9.98	(48.4,-72.4) ± 7.8	M4.2 ± 0.1	12.68 ± 0.03	2.55 ± 0.10	1.6	3.5	—	Magellan/MIKE	20120902
20434114-2433534	12.02	7.76	(56.2,-72.0) ± 1.3	M3.5 ± 0.1	10.41 ± 0.02	0.91 ± 0.08	0.4	3.3	SXD	—	—
21100461-1920302	12.45	7.55	(85.1,-96.4) ± 2.1	M4.2 ± 0.2	10.29 ± 0.02	0.15 ± 0.21	5.1	2.6	SXD	Magellan/MIKE	20110614
21100535-1919573	11.09	7.20	(88.6,-92.5) ± 1.2	M3.0 ± 0.2	9.86 ± 0.02	0.77 ± 0.11	2.7	2.6	SXD	Magellan/MIKE	20110614
21103147-2710578	13.72	9.41	(70.6,-72.3) ± 2.3	M4.4 ± 0.2	12.16 ± 0.02	1.81 ± 0.21	4.9	3.1	SXD	—	—
21183375+3014346	10.83	7.79	(58.9,-22.5) ± 1.4	M1.8 ± 0.8	10.33 ± 0.06	1.99 ± 0.29	4.9	3.4	—	Keck/HIRES	20120710
21195885+3039467	15.86	10.65	(41.7,-20.1) ± 3.4	M5.1 ± 0.4	13.51 ± 0.02	2.39 ± 0.41	7.7	4.1	SXD	Magellan/MIKE	20110615
21200779-1645475	13.73	9.30	(62.1,-54.3) ± 2.6	M4.3 ± 0.1	12.01 ± 0.03	1.76 ± 0.09	5.0	3.5	SXD	Keck/HIRES	20120710
21274019+0137137	12.52	7.88	(80.0,-57.6) ± 3.4	M4.0 ± 0.3	10.59 ± 0.02	0.67 ± 0.23	1.6	3.0	SXD	Magellan/MIKE	20110614
21384755+0504518	14.20	9.87	(50.4,-40.2) ± 3.8	M3.9 ± 0.1	12.55 ± 0.02	2.71 ± 0.10	4.5	3.9	SXD	—	—
22010456+2413016	19.59	12.07	(51.4,-24.2) ± 6.3	M7.9 ± 0.2	15.12 ± 0.02	2.04 ± 0.08	1.8	4.0	SXD	Keck/HIRES	20120710
22085034+1144131	13.45	9.04	(89.8,-50.8) ± 3.2	M4.4 ± 0.1	11.77 ± 0.02	1.42 ± 0.11	1.7	2.9	—	Magellan/MIKE	20101231
22334687-2950101	18.52	11.97	(54.7,-46.2) ± 4.8	M7.4 ± 0.2	14.95 ± 0.03	2.08 ± 0.05	4.2	4.0	SXD	Magellan/MIKE	20110615
22440873-5413183	12.38	8.47	(70.9,-60.1) ± 8.7	M2.8 ± 0.4	11.09 ± 0.03	2.13 ± 0.25	13.1	3.3	—	Magellan/MIKE	20101230
22500768-3213155	16.07	11.58	(69.4,-64.8) ± 11	M6.3 ± 0.3	14.42 ± 0.03	2.17 ± 0.18	13.5	3.4	SXD	Keck/HIRES	20120710
23010610+4002360	18.77	12.28	(73.4,-19.0) ± 4.4	M7.3 ± 0.2	15.23 ± 0.02	2.40 ± 0.09	6.7	3.5	SXD	—	—
23224604-0343438	15.08	10.48	(63.8,-41.2) ± 3.5	M4.6 ± 0.1	13.24 ± 0.03	2.66 ± 0.09	3.8	3.8	—	Magellan/MIKE	20101230

Table 1—Continued

2MASS J	P_{USNOB} (mag)	K_s (mag)	μ (mas/yr)	SpT _{SED}	m_{bol} (mag)	Dm_{phot} (mag)	ΔP_M (mas/yr)	DM_{kin} (mag)	IR Spec. ^a	Opt. Spec.	UT date (yyyy-mm-dd)
23301129-0237227	14.23	9.77	(100.2,-69.7) ± 3.4	M5.6 ± 0.2	12.62 ± 0.02	0.98 ± 0.15	5.0	2.8	SXD	—	—
23314492-0244395	13.31	8.67	(93.6,-66.6) ± 3.4	M4.5 ± 0.3	11.42 ± 0.03	0.95 ± 0.25	6.1	2.9	SXD	Magellan/MIKE	20101231
23323085-1215513	9.83	6.57	(137.9,-81) ± 1.0	M2.4 ± 0.2	9.17 ± 0.03	0.47 ± 0.09	5.7	2.2	—	Magellan/MIKE	20101231
23355015-3401477	16.51	10.76	(88.1,-55.6) ± 10.0	M6.2 ± 0.5	13.63 ± 0.03	1.44 ± 0.37	5.5	3.1	SXD	Magellan/MIKE	20110615

^aIRTF's SXD mode: 0.8-2.4 μm. See Table 2 for log of observations.^bNIR SpT indicates M9 (Allers & Liu 2013).^cThis object was observed with SXD by Allers & Liu (2013).^dOptical spectrum appears as early-type SB2, not an M star.

Table 2. NIR Spectroscopy Log

Object 2MASS J	UT date (YYYY-MM-DD)	Slit Width (‘‘)	sec <i>z</i>	<i>N_{exp}</i> × <i>t</i> (s)	S/N (J,H,K)	SpT _{NIR} ^a	Gravity ^a Type
00140580-3245599	2010-11-14	0.8	2.23	8 × 90.0	132, 118, 134	M7	FLD-G
00193931+1951050	2011-07-07	0.3	1.21	10 × 30.0	44, 49, 42	M4	...
00194303+1951117	2011-07-07	0.3	1.18	8 × 45.0	68, 74, 64	M4	...
00274534-0806046	2017-01-05	0.8	1.19	12 × 29.7	47, 60, 68	M6	FLD-G
00570256-1425174	2010-11-11	0.8	1.22	16 × 60.0	125, 117, 93	M6	FLD-G
01351393-0712517	2010-11-15	0.3	1.12	4 × 30.0	79, 57, 38	M4	...
02241739+2031513	2010-10-05	0.8	1.03	6 × 60.0	106, 111, 104	M6	INT-G
02485260-3404246	2010-11-15	0.3	1.69	6 × 60.0	73, 49, 30	M5	INT-G
02495639-0557352	2010-10-05	0.8	1.17	8 × 60.0	191, 200, 194	M6	VL-G
03363144-2619578	2010-10-05	0.8	1.48	6 × 60.0	301, 312, 296	M6	VL-G
03370343-3042318	2010-10-05	0.8	1.66	8 × 60.0	41, 40, 40	M6	FLD-G
03550477-1032415	2010-11-11	0.8	1.23	16 × 60.0	116, 122, 112	M8	INT-G
04232720+1115174	2010-11-11	0.8	1.21	16 × 60.0	214, 214, 190	M5	VL-G
18011345+0948379	2012-07-05	0.3	1.05	8 × 30.0	104, 108, 90	M5	INT-G
18224692+6723001	2011-07-21	0.8	1.74	10 × 120.0	83, 79, 76	M7	FLD-G
18471351-2808558	2011-07-07	0.8	1.52	8 × 120.0	95, 91, 86	M6	VL-G
18504473-2353389	2011-07-07	0.8	1.38	8 × 120.0	67, 72, 59	<M4	...
19033299-3847058	2011-07-07	0.8	1.92	8 × 120.0	155, 148, 131	<M4	...
19082110+2129364	2012-07-05	0.3	1.01	16 × 120.0	19, 24, 21	<M4	...
19082195-1603249	2011-07-07	0.8	1.26	10 × 120.0	112, 106, 97	M6	VL-G
19472175+3954072	2011-07-07	0.8	1.08	10 × 60.0	173, 187, 151	<M4	...
19533169-0707001	2010-11-18	0.5	1.61	6 × 60.0	245, 230, 190	M4	...
19571814+6242573	2010-11-18	0.5	1.51	6 × 120.0	135, 141, 139	M5	FLD-G
19572094+6242559	2010-11-18	0.5	1.55	6 × 120.0	84, 88, 89	M6	FLD-G
20085368-3519486	2012-07-05	0.3	1.76	8 × 15.0	80, 81, 62	M4	...
20200623-3433203	2010-11-14	0.8	2.09	8 × 90.0	157, 141, 144	M5	FLD-G
20285054+2141119	2012-07-05	0.3	1.01	6 × 30.0	72, 74, 60	<M4	...
20333759-2556521	2011-07-08	0.3	1.46	10 × 60.0	123, 130, 114	M5	INT-G
20434114-2433534	2011-07-08	0.3	1.44	8 × 30.0	104, 121, 107	M4	...
21100461-1920302	2011-07-08	0.3	1.35	8 × 30.0	105, 103, 85	M5	VL-G
21100535-1919573	2011-07-08	0.3	1.37	8 × 30.0	163, 194, 172	<M4	...
21103147-2710578	2011-07-08	0.3	1.49	8 × 60.0	48, 53, 49	M5	INT-G
21195985+3039467	2010-07-17	0.8	1.33	6 × 60.0	146, 116, 81	M5	FLD-G
21374019+0137137	2011-07-08	0.3	1.11	8 × 30.0	117, 123, 104	M5	INT-G
21384755+0504518	2011-07-08	0.3	1.12	8 × 60.0	59, 66, 60	M4	...
22010456+2413016	2011-07-08	0.8	1.08	8 × 120.0	32, 35, 36	M8	FLD-G
22334687-2950101	2010-07-17	0.8	1.60	8 × 60.0	118, 123, 122	M7	VL-G
22500768-3213155	2010-11-14	0.8	1.64	8 × 90.0	189, 172, 155	M4	...
23010610+4002360	2011-07-07	0.8	1.17	12 × 120.0	65, 62, 61	M7	VL-G
22500768-3213155	2010-10-05	0.5	1.74	6 × 90.0	263, 278, 262	M5	FLD-G
23314492-0244395	2011-07-08	0.3	1.08	8 × 60.0	165, 168, 144	M5	INT-G
23355015-3401477	2010-11-11	0.8	1.70	16 × 60.0	157, 105, 80	M6	VL-G

^aStars with SpTs earlier than M4 are outside the valid range of the AL13 NIR spectral typing method. Uncertainty in the IR spectral types is ± 1 subclass as discussed in AL13. Stars with SpTs earlier than M5 cannot be classified with the AL13 NIR gravity classification.

Table 3. Results of Optical Spectroscopy and Membership Assessments

Table 3—Continued

Name	SpT Spec	SpT Source (ref)	RV ^a (km/s)	ΔRV ^b (km/s)	Binary? (Ref) ^c	EW[L _i] ^d (Å)	EW[H _α] ^d (Å)	UVW ^e (km/s)	XZY ^e (pc)	RV, H _α , Li _f Assessment	BPMG Membr. ^g	Prev. Ref. ^g
18420483-5554126	M4.5	Opt (C)	0.43 ± 0.85	0.86	—	0.39	-6.26	(-9.1,-16,-9.1)	(50.4,-18.6,-20.5)	YYY	Y	9
18420694-5554254	M3.5	Opt (C)	1.17 ± 0.17	1.6	<0.05	-7.84	(-8.7,-17.5,-9.1)	(48.2,-17.8,-19.7)	YY?	Y	1	
18435838-3550956	M4.5	Opt (B)	-5.19 ± 2.12	2.21	0.59	-16.62	(-8.3,-14.9,-11.3)	(58.5,0.6,-14.8)	YYY	Y		
18471351-2808555	M6	IR (A)	-7.46 ± 1.65	2.43	0.64	-7.53	(-7.2,-17.2,-8.3)	(55.9,6.9,-11.5)	YYY	Y		
18504473-2353389	—	Opt (B)	-28.39 ± 0.38	-8.29	<0.05	-3.99	(-11.9,-23.5,-12.6)	(7.4,-24.7.9)	NN?	N		
1850451+4259510	M4.1	Opt (B)	11.09 ± 0.24	17.22	<0.05	0.3	(6.2,-16.7,-14.8)	(32.8,-1,-11.2)	NN?	N		
19033299-3847058	M4.3	Opt (B)	4.85 ± 0.81	24.52	<0.05	1.63	(5.9,2,-5,-6)	(33.6,-46.2,-6.1)	NN?	N		
19082110+2129364	K7.5	Opt (B)	-9.09 ± 0.76	3.9	0.53	-7.96	(-6.6,-14.4,-10.2)	(58.1,21.5,-11.9)	YYY	Y		
19082195-1633249	M5.4	Opt (B)	-34.38 ± 0.97	-14.56	<0.05	1.52	(-17,-28,-8,-11)	(34.1,-52.6,-7.7)	NN?	N		
19103951+2436150	K8.5	Opt (B)	-7.52 ± 0.68	12.38	<0.05	1.37	(-4.7,-5.1,-6.4)	(22.4,-41.8,-6.8)	NN?	N		
19153643+2920117	M0.0	Opt (B)	20.32 ± 1.03	39.9	<0.05	1.31	(11.1,-17.8,-5.8)	(18.3,-31.3,-3.3)	NN?	N		
19234424+2629030	K7.8	Opt (B)	18.33 ± 0.81	37.93	<0.05	1.26	(7.6,17.5,-5.5)	(30.6,-54.9,-6)	NN?	N		
19242697+2716351	—	Opt (C)	-4.49 ± 0.32	2.52	<0.05	-13.84	(-7.4,-16.5,-9.4)	(51.1,-3.4,-20.1)	YY?	Y	8	
19243494-3442392	M4.0	Opt (C)	-1.33 ± 2.51	-0.67	SB2	0.15	(-11,-15.9,-9.5)	(41.2,-11.8,-21.4)	YYY	Y		
19260075-5331269	M2.2	Opt (H)	-32.22 ± 1.01	-12.56	—	0.06	1.74	(-14.6,-27.7,-9.8)	(15.8,-36.2,-5.2)	NN?	N	
19275844+3309439	K8.0	Opt (B)	-5.17 ± 0.95	3.29	<0.05	-6.17	(-6.8,-15.7,-9.9)	(58.2,-9.6,-22.4)	YY?	Y		
19300396-2939322	M3.9	Opt (B)	-5.08 ± 0.88	3.48	<0.05	-16.8	(-7,-15.5,-10.6)	(57.6,10.9,-23.3)	YY?	Y	10	
19355395-2846343	M9	IR (A)	1.38 ± 0.50	20.66	<0.05	1.77	(-3.3,-5.5,-6.9)	(16.7,-51.7,-7.2)	NN?	N		
19410321+3806321	M3.7	Opt (B)	-35.12 ± 2.00	-16.05	SB2	<0.05	0.39	(-18.1,-30.8,-6.9)	(16.2,-57.6,-7.7)	NN?	N	
19472175+3954072	—	IR (A)	—	—	SB2	-	(-6.3,-15.3,-11.3)	(53.2,-8.2,-27.3)	YY?	Y		
19533169-0707001	M4	Opt (B)	-2.56 ± 0.69	4.33	SB2	-6	<0.05	-6.48	(-6.3,-15.3,-11.3)	YY?	Y	2, 11
19560294-32207186	M3.7	Opt (B)	—	—	SB2	-6	<0.05	—	(53.2,-8.2,-27.3)	YY?	Y	
19572094+6242559	M5	IR (A)	—	—	—	—	—	—	???	N		
20013718-3313139	M1.0	Opt (C)	-3.71 ± 0.29	2.66	—	0.13	-1.69	(-7.1,-16.7,-9.4)	(55.7,-6,-29.9)	YYY	Y	
20034245+1432215	M1.0	Opt (B)	-15.60 ± 0.73	1.58	<0.05	1.47	(-4.9,-17.7,-8.3)	(36.4,-50.7,-9.6)	NN?	N		
20083784-2545256	M4.7	Opt (B)	-5.74 ± 1.57	2.58	0.22	-5.5	(-6.9,-16.5,-9.2)	(51.2,-15.2,-27.9)	YYY	Y		
20085368-3519486	M4.0	Opt (B)	-3.73 ± 0.25	1.73	<0.05	-6.7	(-8.9,-15.5,-10.5)	(39.2,-4.1,-23.1)	YY?	Y		
20100002-2801410	M3.0	Opt (C)	-8.56 ± 0.44	-0.94	SB2	<0.05	-9.52	(-11.2,-15.8,-9.1)	(46.8,-11.8,-26.3)	YY?	Y	1
20200623-3433293	M5	IR (A)	—	—	—	—	—	—	???	N		
20285054+2141119	M2.5	Opt (B)	-3.25 ± 0.36	13.61	<0.05	-2.23	(-3.2,-4.5,-12)	(19.1,-38.6,-7.5)	NN?	N		
20333759-2556521	M5	IR (A)	-8.48 ± 0.52	-1.27	0.47	-9.44	(-10.8,-17,-8.5)	(36.4,-12,-24.9)	YYY	Y	1	
20385687-4118285	M4.3	Opt (H)	-1.32 ± 1.62	1.2	<0.05	-1.12	(-10.4,-13.6,-11.6)	(48.1,0.1,-36.4)	NN?	N		
20390476-4117390	M3.3	Opt (H)	4.09 ± 0.53	6.61	<0.05	-6.73	(-8.6,-16.1,-12.9)	(39.9,0.1,-30.2)	YY?	Y		
20434114-2433534	M4	IR (A)	-5.0 ± 0.6 ¹	2.12	VB -7	<0.05 ¹	(-8.5,-15.4,-10.5)	(35.1,13.2,-26.1)	YY?	Y	1	
21100461-1920302	M5	IR (A)	-3.97 ± 1.85	3.14	<0.05 ¹	-6.68	(-7.6,-15.5,-11.3)	(22.5,12.6,-20.8)	YY?	Y	9	
21100535-1919573	M2.0	Opt (C)	-5.58 ± 0.19	1.53	<0.05	-2.83	(-9.3,-15.6,-10.5)	(22.5,12.6,-20.8)	YY?	Y	1	
21103147-2710578	M5	IR (A)	-4.21 ± 0.33	0.51	-10.23	(-9.9,-14.9,-9.9)	(29.5,10.4,-27.5)	YY?	Y	8		
21105000-3014346	M0.0	Opt (B)	-22.47 ± 0.81	-7.37	<0.05	-2.66	(-10.6,-23.4,-7.8)	(10.45,5,-11)	NN?	N		
21195985+3039467	M5	IR (A)	—	—	—	—	—	—	???	N		
21200779-1645475	M3.9	Opt (B)	-5.10 ± 0.62	2.07	<0.05	-3.86	(-9.6,-14.3,-10.8)	(31.9,21.1,-32.4)	YY?	Y	12	
21374019+0137137	M5	IR (A)	-15.1 ± 5.0	-5.03	VB -9	<0.05	(-12.6,-19.4,-6.5)	(17.9,-27.1,-23)	YY?	Y		
21384755+0504518	M4	IR (A)	-16.14 ± 1.11	-5.5	SB3	<0.05	-4.83	(-11.4,-20.8,-6.5)	(25.1,43.7,-33.2)	YY?		
22010456+2413016	M8	IR (A)	—	—	—	—	—	—	???	N		
22085034+1144131	M4.3	Opt (B)	-9.26 ± 1.45	0.51	<0.05	-4.96	(-10.2,-15.5,-9.5)	(9.6,29.8,-21.6)	YY?	Y		
22334687-2950101	M7	IR (A)	-1.94 ± 0.30	-2.41	0.65	-22.18	(-10.6,-17.4,-7)	(30.1,0.7,-54.5)	YY?	N		
22440873-5413183	M4.0	Opt (C)	-0.20 ± 0.62	-6.28	<0.05	-6.82	(-11.8,-16.1,-2.5)	(24.1,-11.3,-37.1)	YY?	N		
22500768-3213155	M4	IR (A)	-16.87 ± 0.42	-6.73	—	-	(-9.7,-22,-5.8)	(-9.1,46.7,-15.6)	NN?	N		
23010610+4002360	M7	IR (A)	-11.12 ± 1.88	-9.66	0.62	-8.88	(-11.1,-20.8,-0.9)	(6.8,29.3,-49)	YY?	N		
23224604-0343438	—	—	—	—	<0.05	-15.62	—	—	???	N		

Table 3—Continued

Name	Sp.T Spec	Sp.T Source (ref)	RV ^a (km/s)	Δ RV ^b (km/s)	Binary? (Ref) ^c	EW[L _i] ^d (Å)	EW[H _α] ^d (Å)	UVW ^e (km/s)	XYY ^e (pc)	RV, H _α , Li ^f Assessment	BPMG Membr. ^g	Prev. Ref. ^g
23301129-0237227	M5	IR (A)	—	—	—	—	—	—	—	???	N	
23314492-0244395	M5	IR (A)	-5.44 ± 0.19	-4.47	<0.05	-14.22	(-9.4,-18.6,-5.5)	(2.9,19.3,-32.6)	YY?	Y	Y	1
23323085-1215513	M0,o	Opt (C)	1.38 ± 0.37	0.42	0.16	-1.53	(-10.6,-15.4,-9.5)	(4.2,10.2,-25.2)	YYY	Y	Y	13
23355015-3401477	M6	IR (A)	5.9 ± 0.78	0.62	0.62	-8.42	(-9.2,-16.8,-9.7)	(12.6,1.2,-39.8)	YYY	Y		

^aH For the few targets we were unable to get reliable SpT_{spec}, we include literature values (SpTs in *italics*). Source and references for these are: A: using methods of Allers & Liu (2013), this work; B: using narrow TIO band index defined by Shkolnik et al. (2009); C: using TIO5 band index from Riaz et al. (2006); D: Gagné et al. (2015a); E: TIO band index from Alonso-Floriano et al. (2015b); F: Schlieder et al. (2012a); G: Lépine et al. (2013); H: spectral fitting following the method of Kraus et al. (2014), this work.

^aSystemic RVs are reported for the SBs.

$$b \Delta RV = RV_{obs} - RV_{kin}$$

^c Literature references for binarity: 1: Nicholson (2015), 2: Malo et al. (2014a), 3: Liu et al. (2010), 4: Reiners et al. (2010), 5: Bergfors et al. (2010), 6: Elliott et al. (2014), 7: Shkolnik et al. (2009), 8: Janson et al. (2014), 9: Bowler et al. (2015a).

^dUncertainties in the EW of Li are typically less than 0.05 Å and for H_α are 0.1 Å.

^eUVWs and XYYs are not reported for non-members as the kinematic distance used in the calculations of these values is meaningless if not actual members.

^fYes (Y), No (N), or uncertain (?) membership assessments of the RV, H_α emission and Li absorption.

^gThe first references to list these targets as BPMG members: 1: Malo et al. (2013), 2: Lépine & Simon (2009), 3: Gagné et al. (2015b), 4: Kiss et al. (2011), 5: Shkolnik et al. (2012), 6: Binks & Jeffries (2016), 7: Schlieder et al. (2010), 8: Malo et al. (2014a), 9: Elliott et al. (2016), 10: Liu et al. (2016), 11: Elliott et al. (2014), 12: Schlieder et al. (2012a), 13: Torres et al. (2008)

^hThese SBs have systems RVs consistent with the BPMG, strong H_α emission and inconclusive Li observations. To avoid biasing the sample away from SBs, we designate them 'Y?'. These systems should be followed up for full orbital solutions and/or parallaxes to better understand their ages.

ⁱSchlieder et al. (2010) report an RV of 10.4 ± 2.0 km/s and a ΔRV of 3.8 km/s and thus consider this a likely BPMG member.

^jBinks & Jeffries (2016) report H_α in absorption and thus reject this star as a BPMG member.

^kNIR SpT indicates M9 (Allers & Liu 2013).

^lRV, H_α and/or Li data from the literature: 05061292+0439272 (Alcalá et al. 1996; Alcalá et al. 2000; Lépine et al. 2013); 06352229-5737349 (Kordopatis et al. 2013); 20434114-2433334 (Shkolnik et al. 2012, 2009).

Table 4. Known Members from the Literature + New Members from This Work

Table 4—Continued

2MASS J	Other Name	Ref	Sp-T	Ref	EW[H α] (Å)	Ref	EW[Li] (mA)	Ref	RV (km/s)	Ref	Grav. Type	Ref	π (mas)	Ref	RV, H α , Li Assessment for Ks & Ms ^a	BPMG Memb.?
05200029+0613036	TYC 112-917-1	14	K4	33	-0.2	46	470	33	19.0 ± 0.2	33	"	"	"	"	YYY	Y
05203182+0616115	TYC 112-1486-1	14	K4	33	-0.9	46	510	33	18.0 ± 0.5	33	"	"	"	"	YYY	Y
05241914-1601153		2	M4.9	27	-11.8	8	217	8	17.5 ± 0.6	5	"	"	"	"	YYY	Y
05270147-1154033	AF Lep	1	F7	1	3.9	47	135	47	20.2 ± 0.5	47	"	"	"	"	37.4 ± 0.3	65
05294468-3239141	SCR J0529-3239	17	M4.5	34	-10.0	34	"	"	"	"	"	"	"	"	38.2 ± 1.6	17
05335981-0221325		5	M2.9	27	-6.0	8	i49	8	20.9 ± 0.2	5	"	"	"	"	-Y-	Y?
05471708-5103594	β Pic	1	A3.5	5	-5.1	34	i28	21	22.5 ± 0.2	5	"	"	"	"	51.4 ± 0.1	67
06131330-2742054	SCR J0613-2742 AB	2	M3.5	5	-0.5	31	420	31	16.3 ± 0.8	31	"	"	"	"	34.0 ± 1.0	17
06182824-7202416	AO Men	1	K6.5	1	"	"	"	"	"	"	"	"	"	"	25.6 ± 0.2	65
08173943-8243298		5	M4	5	-7.6	34	"	"	15.6 ± 1.5	5	"	"	"	"	YY-	Y
08228744-5726530		5	M4.5+>L0	5	-7.3	34	"	"	14.7 ± 0.2	5	"	"	"	"	YY-	Y
09360429+3733104	HD 82939	13	G5	35	"	"	"	"	-1.0 ± 0.3	56	"	"	"	"	25.6 ± 0.3	65
09361593+3731456	HIP 47133	18	M2	20	0.0	44	"	"	-2.5 ± 1.0	20	"	"	"	"	26.3 ± 0.3	65
101411918+2104297	HIP 50156	8	M0.7	36	-1.0	36	i20	8	2.7 ± 0.1	29	"	"	"	"	43.3 ± 1.8	67
10172689-5324625	TWA 22	37	M5	37	-8.3	11	510	11	14.8 ± 2.1	37	"	"	"	"	57.0 ± 0.7	37
10593834+2526155	BD+26 2161	13	K4	38	"	"	"	"	"	"	"	"	"	"	--	--
10593870+2526138	BD+26 2161B	20	K5	20	"	"	"	"	-3.5 ± 0.3	20	"	"	"	"	46.8 ± 0.4	65
13545390-1341011		2	M1	5	-4.7	34	560	31	13.4 ± 1.3	31	"	"	"	"	47.5 ± 0.4	65
14141190-1521125		5	M2.5	5	-3.3	34	"	"	5.7 ± 0.2	5	"	"	"	"	YY-	Y
141412141-1521215		9	M3.5	39	"	"	"	"	-21.6 ± 99.0	39	"	"	"	"	N--	Y?
14253913-4113323		2	K5	2	-2.3	34	"	"	-4.1 ± 1.5	59	"	"	"	"	33.1 ± 4.9	67
15385679-5742190	HD 139084 B	21	M2.5	21	-7.0	17	685	21	-1.2 ± 1.3	5	"	"	"	"	14.4 ± 1.0	17
15385737-5742273	V343 Nor	11	M5	16	-4.4	11	460	31	0.1 ± 2.0	31	"	"	"	"	YY-	Y
16181789-2836502	HIP 79881	1	K0	1	"	"	"	"	292	31	4.2 ± 1.4	31	"	"	27.1 ± 0.3	65
16430128-1754274		7	M0.6	1	"	"	"	"	-13.0 ± 0.8	60	"	"	"	"	24.2 ± 0.2	67
1657229-5343316		5	M3	27	-2.1	8	364	8	-10.0 ± 1.5	8	"	"	"	"	YY-	Y
171505219-3333398		5	M0	5	-2.5	34	"	"	1.4 ± 0.2	5	"	"	"	"	19.4 ± 0.7	65
CD-27 11535		14	K5	5	-3.0	34	"	"	-14.6 ± 3.5	5	"	"	"	"	YY-	Y?
17172550-6657039	V824 Ara	1	M4.5	14	-4.2	31	490	31	-6.4 ± 0.8	31	"	"	"	"	13.1 ± 0.6	65
17173128-6657055	HD 155555C	1	M4.5	1	-5.5	31	250	31	5.9 ± 0.2	61	"	"	"	"	32.8 ± 0.4	65
17292067-5014529	GSC8350-1924	16	M3	16	-6.7	34	50	20	2.7 ± 1.8	31	"	"	"	"	YY?	Y
CD-54 7336		16	K1	16	0.2	48	360	31	-0.1 ± 0.9	5	"	"	"	"	YY?	Y
HD 160305	7	F9	16	0	2.6	7	130	7	2.4 ± 1.1	7	"	"	"	"	14.4 ± 0.2	65
1717503-5043279		14	K5	14	-4.2	31	490	31	-6.4 ± 0.8	31	"	"	"	"	YY-	Y
17483374-5306433	HD 161460	16	K0	16	0.4	48	320	31	1.4 ± 0.8	31	"	"	"	"	YY	Y?
18030341-5138564	HD 164249	1	F5	1	"	"	"	"	107	31	0.5 ± 0.4	31	"	"	YY?	Y
18030409-5138561	HD 164249 B	16	M2	16	-2.3	31	70	31	-2.4 ± 1.3	31	"	"	"	"	YY?	Y
18064990-4325297	HD 165189	1	A5	1	"	"	"	"	-7.8 ± 0.4	60	"	"	"	"	23.9 ± 0.7	67
181414047-3247344	V4046 Sgr	16	K6	16	-60.0	49	440	53	-13.3 ± 7.7	5	"	"	"	"	YY	Y?
18420483-5554126		16	M4.5	16	-3.1	34	200	31	-5.7 ± 0.8	31	"	"	"	"	YY-	Y
18453269-5554254	HD 172555	5	M3	5	-5.0	22	i46	22	0.3 ± 3.6	5	"	"	"	"	35.0 ± 0.2	67
18463575-6451460	CD-64 1208	1	K7	1	"	"	"	"	290	31	-7.0 ± 2.6	31	"	"	YY	Y
TYC 9703-0762		16	M1	16	-1.9	530	31	-13.8 ± 0.8	31	"	"	"	"	13.2 ± 3.8	67	
		22	F5	22	"	"	"	"	"	"	"	"	"	"	YY-	Y
		107		22	"	"	"	"	"	"	"	"	"	"	19.8 ± 0.3	65

Table 4—Continued

Table 4—Continued

2MASS J	Other Name	Ref	Sp-T	Ref	EW[H α] (Å)	Ref	EW[L β] (mA)	Ref	RV (km/s)	Ref	Grav. Type	Ref	π (mas)	Ref	RV, H α , Li Assessment for Ks & Ms ^a	BFMG Memb. for Ks & Ms ^a
New Members																
00164976+4515417		69	M4.5	69	-7.3	69	<50	69	-12.1 ± 0.6	69	Y? Y?	Y?
00193381+1951050		69	M4.5	69	-6.8	69	120	69	-7.0 ± 0.4	69	YYY	Y?
00194303+1951117		69	M4.7	69	-5.1	69	<50	69	-6.7 ± 0.3	69	YY?	Y?
00281434-3227556		69	M4.3	69	-10.6	69	378	69	6.8 ± 2.7	69	YYY	Y
00413538-5621127		69	M7.9	69	-34.1	69	134	69	6.6 ± 1.8	69	YYY	Y
00482667-1847204		69	M4.6	69	-6.6	69	530	69	7.2 ± 0.7	69	YYY	Y
00501752+0837341		69	M3.9	69	-4.8	69	150	69	2.1 ± 2.0	69	YY	Y
01303534+208393		69	M4.7	69	-8.1	69	<50	69	-2.8 ± 0.9	69	Y? Y?	Y?
02241739+2031513		69	M5.8	69	-10.7	69	680	69	8.6 ± 1.2	69	INT-G	69	YYY	Y
02335984-1811525		69	M2.9	69	-4.6	69	<50	69	12.0 ± 1.2	69	YY?	Y
02450826-0708120		69	M4.1	69	-8.3	69	460	69	11.4 ± 2.3	69	YYY	Y
02485260-3404246		69	M3.9	69	-7.0	69	<50	69	14.8 ± 0.5	69	INT-G	69	YY?	Y?
02495639-0557352		69	M5.9	69	-11.6	69	590	69	14.4 ± 0.4	69	VL-G	69	YYY	Y
03255277-3601161		69	M4.5	69	-6.2	69	<50	69	16.6 ± 2.4	69	YY?	Y
03363144-2619575		69	M6.1	69	-11.2	69	330	69	16.6 ± 2.7	69	VL-G	69	YYY	Y
03370343-3042318		69	M6.4	69	-10.3	69	560	69	11.9 ± 3.5	69	FLD-G	69	Y? YY	Y?
03393700+4531160		69	M3.5	69	-4.6	69	<50	69	7.7 ± 2.0	69	YY?	Y?
03550477-1032415		69	M8.9	69	-7.0	69	920	69	17.0 ± 0.7	69	INT-G	69	YYY	Y
04232720+1115174		69	M5.7	69	-4.1	69	580	69	14.3 ± 0.4	69	VL-G	69	YYY	Y
05015665+0108429		69	M3.6	69	-4.9	69	<50	69	18.6 ± 0.5	69	YY?	Y?
05061292+0439272		69	M3.8	69	-6.2	69	270	69	18.8 ± 2.4	69	YYY	Y
05363846+1117487		69	M3.2	69	-2.5	69	<50	69	20.7 ± 0.4	69	Y? YY?	Y?
13215631-1052098		69	M4.2	69	-5.6	69	<50	69	-4.0 ± 2.1	69	YY?	Y
15063505-3639297		69	M4.8	69	-12.6	69	780	69	0.0 ± 1.8	69	YYY	Y
18011345+0948379		69	M4.0	69	-11.4	69	150	69	-22.9 ± 1.7	69	INT-G	69	YYY	Y
18055491-5704307		69	M3.6	69	-6.1	69	<50	69	-0.6 ± 0.4	69	YY?	Y
18090694-7613239		69	M5.6	69	-8.3	69	600	69	7.0 ± 0.4	69	YYY	Y
18092970-5430532		69	M5.6	69	-8.2	69	560	69	-2.0 ± 0.8	69	YYY	Y
18435838-3559096		69	M4.5	69	-16.6	69	590	69	-5.2 ± 2.1	69	YYY	Y
18471351-2808558		69	M5.1	69	-7.5	69	640	69	-7.5 ± 1.6	69	VL-G	69	YYY	Y
19082195-1603249		69	M6.8	69	-8.0	69	530	69	-9.1 ± 0.8	69	VL-G	69	YYY	Y
19260075-5331269		69	M4.2	69	-2.9	69	150	69	-1.3 ± 2.5	69	YYY	Y
19300396-2939322		69	M4.2	69	-6.2	69	<50	69	-5.2 ± 1.0	69	YY?	Y
20083784-2545256		69	M4.7	69	-5.5	69	220	69	-5.7 ± 1.6	69	YYY	Y
20085368-3519486		69	M3.6	69	-6.7	69	<50	69	-3.7 ± 0.2	69	YY?	Y
21200779-1645475		69	M4.3	69	-3.9	69	<50	69	-5.1 ± 0.6	69	YY?	Y
21384755+0504518		69	M3.9	69	-4.8	69	<50	69	-16.1 ± 1.1	69	YY?	Y
22085034+1144131		69	M4.4	69	-5.0	69	<50	69	-9.3 ± 1.4	69	YY?	Y
22334687-2950101		69	M7.4	69	-22.2	69	650	69	-1.9 ± 0.3	69	VL-G	69	YYY	Y
23010610+4002360		69	M7.3	69	-8.9	69	620	69	-16.9 ± 0.4	69	VL-G	69	NYY	Y?
23555015-3401477		69	M6.2	69	-8.4	69	620	69	5.9 ± 0.8	69	VL-G	69	YYY	Y

^aThe last two columns list the assessment of each age diagnostic and membership status following the prescription of this paper as summarized by Figure 3. We subjected the 113 published members with K and M spectral types to the same tests described in Sections 3–5. The results of those tests are summarized in the text.

Note. — Refs: 1: Zuckerman et al. (2001b), 2: Malo et al. (2013), 3: Lépine & Simon (2009), 4: Gagné & Simon (2014a), 5: Malo et al. (2014a), 6: Gagné et al. (2015a), 7: Kiss et al. (2011).

- 8: Binks & Jeffries (2016), 9: Elliott et al. (2016), 10: Schlieder et al. (2010), 11: Song et al. (2003), 12: Moór et al. (2006), 13: Alonso-Floriano et al. (2015a), 14: Elliott et al. (2014), 15: Rodriguez et al. (2014), 16: Torres et al. (2008), 17: Riedel et al. (2014), 18: Schlieder et al. (2012a), 19: Teixeira et al. (2009), 20: Schlieder et al. (2012b), 21: Malo et al. (2014b), 22: Moór et al. (2013), 23: Liu et al. (2016), 24: Barrado y Navascués et al. (1999), 25: Liu et al. (2013), 26: Allers & Liu (2013), 27: Binks & Jeffries (2014), 28: López-Santiago et al. (2010), 30: Zuckerman & Song (2004), 31: Torres et al. (2006), 32: Kordopatis et al. (2013), 33: Alcalá et al. (2000), 34: Riaz et al. (2006), 35: Houk & Smith-Moore (1988), 36: Shkolnik et al. (2009), 37: Teixeira et al. (2009), 38: Stephenson (1986), 39: Hawley et al. (1997), 40: Hipparcos Catalog, 41: Reid et al. (2008), 42: Cruz et al. (2009), 43: Shkolnik et al. (2012), 44: Lépine et al. (2013), 45: Reid et al. (2007), 46: Alcalá et al. (1996), 47: White et al. (2012), 48: Song et al. (2017), 49: Herbig & Bell (1988), 50: Martin et al. (2010), 51: Gaidos et al. (2014), 52: Reid et al. (2002), 53: da Silva et al. (2001), 54: Kraus et al. (2001), 55: Faherty et al. (2016), 56: Montes et al. (2016), 57: Bailey et al. (2012), 58: Macintosh et al. (2015), 59: Gizis et al. (2002), 60: Gorbatchev (2006), 61: Strassmeier & Rice (2000), 62: Wilson (1953), 63: Zuckerman & Webb (2000), 64: Allers et al. (2016), 65: Gaia Collaboration et al. (2016), 66: Faherty et al. (2013), 67: van Leeuwen (2007), 68: Schneider et al. (2017), 69: this work (see Tables 1-3 for more details on these members).

REFERENCES

- Ahn, C. P., et al. 2012, ApJS, 203, 21
- Alcalá, J. M., Covino, E., Torres, G., Sterzik, M. F., Pfeiffer, M. J., & Neuhäuser, R. 2000, A&A, 353, 186
- Alcala, J. M., et al. 1996, A&AS, 119, 7
- Aller, K. M., et al. 2016, ApJ, 821, 120
- Allers, K. N., Gallimore, J. F., Liu, M. C., & Dupuy, T. J. 2016, ApJ, 819, 133
- Allers, K. N., & Liu, M. C. 2013, ApJ, 772, 79
- Alonso-Floriano, F. J., Caballero, J. A., Cortés-Contreras, M., Solano, E., & Montes, D. 2015a, A&A, 583, A85
- Alonso-Floriano, F. J., et al. 2015b, A&A, 577, A128
- Bailey, III, J. I., White, R. J., Blake, C. H., Charbonneau, D., Barman, T. S., Tanner, A. M., & Torres, G. 2012, ApJ, 749, 16, 15 pp
- Baraffe, I., & Chabrier, G. 2010, A&A, 521, A44, 52 pp
- Baraffe, I., Homeier, D., Allard, F., & Chabrier, G. 2015, A&A, 577, A42
- Barrado Y Navascués, D. 2006, A&A, 459, 511
- Barrado y Navascués, D., & Martín, E. L. 2003, AJ, 126, 2997
- Barrado y Navascués, D., Stauffer, J. R., & Jayawardhana, R. 2004, ApJ, 614, 386
- Barrado y Navascués, D., Stauffer, J. R., & Patten, B. M. 1999, ApJ, 522, L53
- Bell, C. P. M., Mamajek, E. E., & Naylor, T. 2015, MNRAS, 454, 593
- Bergfors, C., et al. 2010, A&A, 520, A54
- Binks, A. S., & Jeffries, R. D. 2014, MNRAS, 438, L11
- . 2016, MNRAS, 455, 3345
- Boccaletti, A., et al. 2015, Nature, 526, 230

- Bochanski, J. J., Hawley, S. L., Covey, K. R., West, A. A., Reid, I. N., Golimowski, D. A., & Ivezić, Ž. 2010, AJ, 139, 2679
- Bouvier, J. 2008, A&A, 489, L53
- Bowler, B. P., Liu, M. C., Shkolnik, E. L., & Dupuy, T. J. 2013, ApJ, 774, 55,12 pp
- Bowler, B. P., Liu, M. C., Shkolnik, E. L., & Tamura, M. 2015a, ApJS, 216, 7
- Bowler, B. P., et al. 2015b, ApJ, 806, 62
- Chabrier, G., Baraffe, I., & Plez, B. 1996, ApJ, 459, L91, 4 pp
- Chabrier, G., Gallardo, J., & Baraffe, I. 2007, A&A, 472, L17
- Chen, Y., Bressan, A., Girardi, L., Marigo, P., Kong, X., & Lanza, A. 2015, MNRAS, 452, 1068
- Chubak, C., Marcy, G., Fischer, D. A., Howard, A. W., Isaacson, H., Johnson, J. A., & Wright, J. T. 2012, ArXiv e-prints
- Cruz, K. L., Kirkpatrick, J. D., & Burgasser, A. J. 2009, AJ, 137, 3345
- Cushing, M. C., Vacca, W. D., & Rayner, J. T. 2004, PASP, 116, 362
- Cutri, R. M., et al. 2003, 2MASS All Sky Catalog of point sources., ed. Cutri, R. M., Skrutskie, M. F., van Dyk, S., Beichman, C. A., Carpenter, J. M., Chester, T., Cambresy, L., Evans, T., Fowler, J., Gizis, J., Howard, E., Huchra, J., Jarrett, T., Kopan, E. L., Kirkpatrick, J. D., Light, R. M., Marsh, K. A., McCallon, H., Schneider, S., Stiening, R., Sykes, M., Weinberg, M., Wheaton, W. A., Wheelock, S., & Zacarias, N.
- da Silva, L., Torres, C. A. O., de La Reza, R., Quast, G. R., Melo, C. H. F., & Sterzik, M. F. 2009, A&A, 508, 833
- Delorme, P., Lagrange, A. M., Chauvin, G., Bonavita, M., Lacour, S., Bonnefoy, M., Ehrenreich, D., & Beust, H. 2012, A&A, 539, A72
- Dobbie, P. D., Lodieu, N., & Sharp, R. G. 2010, MNRAS, 409, 1002
- Elliott, P., Bayo, A., Melo, C. H. F., Torres, C. A. O., Sterzik, M., & Quast, G. R. 2014, A&A, 568, A26
- Elliott, P., Bayo, A., Melo, C. H. F., Torres, C. A. O., Sterzik, M. F., Quast, G. R., Montes, D., & Brahm, R. 2016, A&A, 590, A13

- Epcstein, N., et al. 1994, Ap&SS, 217, 3
- Faherty, J. K., Rice, E. L., Cruz, K. L., Mamajek, E. E., & Núñez, A. 2013, AJ, 145, 2
- Faherty, J. K., et al. 2016, ApJS, 225, 10
- Feiden, G. A. 2016, A&A, 593, A99
- Findeisen, K., & Hillenbrand, L. 2010, AJ, 139, 1338
- Fitzpatrick, M. J. 1993, in Astronomical Society of the Pacific Conference Series, Vol. 52, Astronomical Data Analysis Software and Systems II, ed. R. J. Hanisch, R. J. V. Brissenden, & J. Barnes, 472–+
- Gagné, J., et al. 2015a, ApJS, 219, 33
- Gagné, J., Lafrenière, D., Doyon, R., Malo, L., & Artigau, É. 2015b, ApJ, 798, 73
- Gaia Collaboration, et al. 2016, A&A, 595, A2
- Gaidos, E., et al. 2014, MNRAS, 443, 2561
- Gizis, J. E., Reid, I. N., & Hawley, S. L. 2002, AJ, 123, 3356
- Gontcharov, G. A. 2006, Astronomical and Astrophysical Transactions, 25, 145
- Gray, R. O., Corbally, C. J., Garrison, R. F., McFadden, M. T., & Robinson, P. E. 2003, AJ, 126, 2048
- Hawley, S. L., Gizis, J. E., & Reid, N. I. 1997, AJ, 113, 1458
- Herbig, G. H., & Bell, K. R. 1988, Third Catalog of Emission-Line Stars of the Orion Population : 3 : 1988
- Herczeg, G. J., & Hillenbrand, L. A. 2014, ApJ, 786, 97
- Houk, N., & Smith-Moore, M. 1988, Michigan Catalogue of Two-dimensional Spectral Types for the HD Stars. Volume 4, Declinations -26 deg to -12 deg.0.
- Janson, M., et al. 2014, ApJS, 214, 17
- Kastner, J. H., Zuckerman, B., Weintraub, D. A., & Forveille, T. 1997, Science, 277, 67
- Kelson, D. D. 2003, PASP, 115, 688
- Kenyon, S. J., & Bromley, B. C. 2006, AJ, 131, 1837

- Kirkpatrick, J. D., et al. 2010, ApJS, 190, 100
- Kiss, L. L., et al. 2011, MNRAS, 411, 117
- Kordopatis, G., et al. 2013, The Astronomical Journal, 146, 134
- Kraus, A. L., Cody, A. M., Covey, K. R., Rizzuto, A. C., Mann, A. W., & Ireland, M. J. 2015, ApJ, 807, 3
- Kraus, A. L., Herczeg, G. J., Rizzuto, A. C., Mann, A. W., Slesnick, C. L., Carpenter, J. M., Hillenbrand, L. A., & Mamajek, E. E. 2017, ApJ, 838, 150
- Kraus, A. L., Shkolnik, E. L., Allers, K. N., & Liu, M. C. 2014, AJ, 147, 146, 22 pp
- Lagrange, A.-M., et al. 2010, Science, 329, 57
- Lépine, S., Hilton, E. J., Mann, A. W., Wilde, M., Rojas-Ayala, B., Cruz, K. L., & Gaidos, E. 2013, AJ, 145, 102
- Lépine, S., & Simon, M. 2009, AJ, 137, 3632
- Lissauer, J. J. 1987, Icarus, 69, 249
- Liu, M. C. 2004, Science, 305, 1442
- Liu, M. C., Dupuy, T. J., & Allers, K. N. 2016, ApJ, 833, 96
- Liu, M. C., et al. 2013, ApJ, 777, L20
- Liu, M. C., et al. 2010, in Society of Photo-Optical Instrumentation Engineers (SPIE) Conference Series, Vol. 7736, Society of Photo-Optical Instrumentation Engineers (SPIE) Conference Series
- López-Santiago, J., Montes, D., Crespo-Chacón, I., & Fernández-Figueroa, M. J. 2006, ApJ, 643, 1160
- López-Santiago, J., Montes, D., Gálvez-Ortiz, M. C., Crespo-Chacón, I., Martínez-Arnáiz, R. M., Fernández-Figueroa, M. J., de Castro, E., & Cornide, M. 2010, A&A, 514, A97+
- Macintosh, B., et al. 2015, Science, 350, 64
- Makarov, V. V. 2007, ApJS, 169, 105

- Malo, L., Artigau, É., Doyon, R., Lafrenière, D., Albert, L., & Gagné, J. 2014a, ApJ, 788, 81, 15 pp
- Malo, L., Doyon, R., Feiden, G. A., Albert, L., Lafrenière, D., Artigau, É., Gagné, J., & Riedel, A. 2014b, ApJ, 792, 37
- Malo, L., Doyon, R., Lafrenière, D., Artigau, É., Gagné, J., Baron, F., & Riedel, A. 2013, ApJ, 762, 88, 50 pp
- Mamajek, E. E. 2016, in IAU Symposium, Vol. 314, Young Stars & Planets Near the Sun, ed. J. H. Kastner, B. Stelzer, & S. A. Metchev, 21–26
- Mamajek, E. E., & Bell, C. P. M. 2014, MNRAS, 445, 2169
- Martín, E. L., et al. 2010, A&A, 517, A53
- Mentuch, E., Brandeker, A., van Kerkwijk, M. H., Jayawardhana, R., & Hauschmidt, P. H. 2008, ApJ, 689, 1127
- Messina, S., et al. 2016, A&A, 596, A29
- Monet, D. G., et al. 2003, AJ, 125, 984
- Montes, D., López-Santiago, J., Gálvez, M. C., Fernández-Figueroa, M. J., De Castro, E., & Cornide, M. 2001, MNRAS, 328, 45
- Montet, B. T., et al. 2015, ApJ, 813, L11
- Moór, A., Ábrahám, P., Derekas, A., Kiss, C., Kiss, L. L., Apai, D., Grady, C., & Henning, T. 2006, ApJ, 644, 525
- Moór, A., Szabó, G. M., Kiss, L. L., Kiss, C., Ábrahám, P., Szulágyi, J., Kóspál, Á., & Szalai, T. 2013, MNRAS, 435, 1376
- Naylor, T. 2009, MNRAS, 399, 432
- Nicholson, M. P. 2015, VizieR Online Data Catalog, 1330
- Nidever, D. L., Marcy, G. W., Butler, R. P., Fischer, D. A., & Vogt, S. S. 2002, ApJS, 141, 503
- Nielsen, E. L., et al. 2016, AJ, 152, 175
- Ochsenbein, F., Bauer, P., & Marcout, J. 2000, A&AS, 143, 23

- Ortega, V. G., de la Reza, R., Jilinski, E., & Bazzanella, B. 2002, ApJ, 575, L75
- Palla, F., Randich, S., Pavlenko, Y. V., Flaccomio, E., & Pallavicini, R. 2007, ApJ, 659, L41
- Pecaut, M. J., & Mamajek, E. E. 2013, ApJS, 208, 9
- Pecaut, M. J., Mamajek, E. E., & Bubar, E. J. 2012, ApJ, 746, 154
- Pollack, J. B., Hubickyj, O., Bodenheimer, P., Lissauer, J. J., Podolak, M., & Greenzweig, Y. 1996, Icarus, 124, 62
- Pompéia, L., et al. 2011, MNRAS, 415, 1138
- Reid, I. N., Cruz, K. L., & Allen, P. R. 2007, AJ, 133, 2825
- Reid, I. N., Cruz, K. L., Kirkpatrick, J. D., Allen, P. R., Mungall, F., Liebert, J., Lowrance, P., & Sweet, A. 2008, AJ, 136, 1290
- Reid, I. N., Gizis, J. E., & Hawley, S. L. 2002, AJ, 124, 2721
- Reiners, A., Seifahrt, A., & Dreizler, S. 2010, A&A, 513, L9
- Riaz, B., Gizis, J. E., & Harvin, J. 2006, AJ, 132, 866
- Riedel, A. R., et al. 2014, AJ, 147, 85
- Rizzuto, A. C., Ireland, M. J., Dupuy, T. J., & Kraus, A. L. 2016, ApJ, 817, 164
- Rizzuto, A. C., Ireland, M. J., & Kraus, A. L. 2015, MNRAS, 448, 2737
- Rodriguez, D. R., Bessell, M. S., Zuckerman, B., & Kastner, J. H. 2011, ApJ, 727, 62, 10 pp
- Rodriguez, D. R., Zuckerman, B., Faherty, J. K., & Vican, L. 2014, A&A, 567, A20
- Rodriguez, D. R., Zuckerman, B., Kastner, J. H., Bessell, M. S., Faherty, J. K., & Murphy, S. J. 2013, ApJ, 774, 101
- Schlieder, J. E., Lépine, S., & Simon, M. 2010, AJ, 140, 119
- . 2012a, AJ, 143, 80, 15 pp
- . 2012b, AJ, 144, 109
- Schneider, A. C., Windsor, J., Cushing, M. C., Kirkpatrick, J. D., & Shkolnik, E. L. 2017, AJ, 153, 196

- Shkolnik, E., Liu, M. C., & Reid, I. N. 2009, ApJ, 699, 649
- Shkolnik, E. L., Anglada-Escudé, G., Liu, M. C., Bowler, B. P., Weinberger, A. J., Boss, A. P., Reid, I. N., & Tamura, M. 2012, ApJ, 758, 56, 23 pp
- Shkolnik, E. L., Hebb, L., Liu, M. C., Reid, I. N., & Cameron, A. C. 2010, ApJ, 716, 1522
- Shkolnik, E. L., Liu, M. C., Reid, I. N., Dupuy, T., & Weinberger, A. J. 2011, ApJ, 727, 6, 12 pp
- Skrutskie, M. F., et al. 2006, AJ, 131, 1163
- Soderblom, D. R., Pilachowski, C. A., Fedele, S. B., & Jones, B. F. 1993, AJ, 105, 2299
- Somers, G., & Pinsonneault, M. H. 2014, ApJ, 790, 72
- Somers, G., & Stassun, K. G. 2017, AJ, 153, 101
- Song, I., Zuckerman, B., & Bessell, M. S. 2003, ApJ, 599, 342
- . 2012, AJ, 144, 8
- Stauffer, J. R., Hartmann, L. W., Prosser, C. F., Randich, S., Balachandran, S., Patten, B. M., Simon, T., & Giampapa, M. 1997, ApJ, 479, 776
- Stauffer, J. R., Schultz, G., & Kirkpatrick, J. D. 1998, ApJ, 499, L199+
- Stephenson, C. B. 1986, ApJ, 300, 779
- Strassmeier, K. G., & Rice, J. B. 2000, A&A, 360, 1019
- Teixeira, R., Ducourant, C., Chauvin, G., Krone-Martins, A., Bonnefoy, M., & Song, I. 2009, A&A, 503, 281
- Torres, C. A. O., da Silva, L., Quast, G. R., de la Reza, R., & Jilinski, E. 2000, AJ, 120, 1410
- Torres, C. A. O., Quast, G. R., da Silva, L., de La Reza, R., Melo, C. H. F., & Sterzik, M. 2006, A&A, 460, 695
- Torres, C. A. O., Quast, G. R., Melo, C. H. F., & Sterzik, M. F. 2008, Young Nearby Loose Associations (Handbook of Star Forming Regions, Volume II: The Southern Sky ASP Monograph Publications, Vol. 5. Edited by Bo Reipurth), 757, 56 pp
- Vacca, W. D., Cushing, M. C., & Rayner, J. T. 2004, PASP, 116, 352

- van Leeuwen, F. 2007, A&A, 474, 653
- Webb, R. A., Zuckerman, B., Platais, I., Patience, J., White, R. J., Schwartz, M. J., & McCarthy, C. 1999, ApJ, 512, L63
- White, R. J., Gabor, J. M., & Hillenbrand, L. A. 2007, AJ, 133, 2524
- Wilson, R. E. 1953, Carnegie Institute Washington D.C. Publication
- Zacharias, N., et al. 2010, AJ, 139, 2184
- Zuckerman, B., & Song, I. 2004, ARA&A, 42, 685
- Zuckerman, B., Song, I., Bessell, M. S., & Webb, R. A. 2001a, ApJ, 562, L87
- Zuckerman, B., & Webb, R. A. 2000, ApJ, 535, 959
- Zuckerman, B., Webb, R. A., Schwartz, M., & Becklin, E. E. 2001b, ApJ, 549, L233